



RESEARCH ARTICLE

10.1029/2018MS001571

Special Section:

The Energy Exascale Earth System Model (E3SM)

Key Points:

- We developed a new carbon-nitrogen-phosphorus land model (ELMv1-ECA) integrated in the E3SM Earth system model
- We benchmarked the simulated present-day carbon cycle using the International Land Model Benchmarking package (ILAMB)
- We documented model performance and identified necessary future improvements

Supporting Information:

- Supporting Information S1

Correspondence to:

Q. Zhu,
qzhu@lbl.gov

Citation:

Zhu, Q., Riley, W. J., Tang, J., Collier, N., Hoffman, F. M., Yang, X., & Bisht, G. (2019). Representing nitrogen, phosphorus, and carbon interactions in the E3SM land model: Development and global benchmarking. *Journal of Advances in Modeling Earth Systems*, 11, 2238–2258. <https://doi.org/10.1029/2018MS001571>

Received 21 NOV 2018

Accepted 14 JUN 2019

Accepted article online 22 JUN 2019

Published online 11 JUL 2019

©2019. The Authors.

This is an open access article under the terms of the Creative Commons Attribution-NonCommercial-NoDerivs License, which permits use and distribution in any medium, provided the original work is properly cited, the use is non-commercial and no modifications or adaptations are made.

Representing Nitrogen, Phosphorus, and Carbon Interactions in the E3SM Land Model: Development and Global Benchmarking

Qing Zhu¹ , William J. Riley¹ , Jinyun Tang¹ , Nathan Collier² , Forrest M. Hoffman^{2,3} , Xiaojuan Yang⁴ , and Gautam Bisht¹

¹Climate and Ecosystem Sciences Division, Climate Sciences Department, Lawrence Berkeley National Laboratory, Berkeley, CA, USA, ²Computational Earth Sciences Group and Climate Change Science Institute, Oak Ridge National Laboratory, Oak Ridge, TN, USA, ³Department of Civil and Environmental Engineering, University of Tennessee, Knoxville, TN, USA, ⁴Environmental Sciences Division and Climate Change Science Institute, Oak Ridge National Laboratory, Oak Ridge, TN, USA

Abstract Over the past several decades, the land modeling community has recognized the importance of nutrient regulation on the global terrestrial carbon cycle. Implementations of nutrient limitation in land models are diverse, varying from applying simple empirical down-regulation of potential gross primary productivity under nutrient deficit conditions to more mechanistic treatments. In this study, we introduce a new approach to model multinutrient (nitrogen [N] and phosphorus [P]) limitations in the Energy Exascale Earth System Model (E3SM) Land Model version 1 (ELMv1-ECA). The development is grounded on (1) advances in representing multiple-consumer, multiple-nutrient competition; (2) a generic dynamic allocation scheme based on water, N, P, and light availability; (3) flexible plant CNP stoichiometry; (4) prognostic treatment of N and P constraints on several carbon cycle processes; and (5) global data sets of plant physiological traits. Through benchmarking the model against best knowledge of global plant and soil carbon pools and fluxes, we show that our implementation of nutrient constraints on the present-day carbon cycle is robust at the global scale. Compared with predecessor versions, ELMv1-ECA better predicts global-scale gross primary productivity, ecosystem respiration, leaf area index, vegetation biomass, soil carbon stocks, evapotranspiration, N₂O emissions, and NO₃⁻ leaching. Factorial experiments indicate that representing the phosphorus cycle improves modeled carbon fluxes, while considering dynamic allocation improves modeled carbon stock density. We also highlight the value of using the International Land Model Benchmarking (ILAMB) package to evaluate and document performance during model development.

1. Introduction

Anthropogenic CO₂ emissions since the preindustrial era have increased atmospheric CO₂ concentrations to levels that the Earth has not experienced for hundreds of thousands of years (Petit et al., 1999). Such enhanced atmospheric CO₂ dramatically alters the global energy balance via a positive radiative forcing effect (Myhre et al., 1998). Terrestrial ecosystems currently remove from the atmosphere about a quarter of anthropogenic CO₂ emissions (Houghton, 2007; Le Quéré et al., 2016) via photosynthesis, thus reducing the warming effects on climate. Furthermore, terrestrial ecosystems have the potential to sequester CO₂ more efficiently in the future due to the CO₂ fertilization effect (Mao et al., 2016; Norby et al., 2005).

However, this potential benefit from terrestrial ecosystems may be limited because a larger terrestrial CO₂ sink requires a greater supply of essential nutrients, particularly nitrogen (N) and phosphorus (P) (Falkowski et al., 2000). Although human activities have enhanced global N and P availability (e.g., from agricultural fertilization and fossil fuel combustion; Galloway et al., 2004; Vitousek et al., 1997), at the global scale these increases are unlikely to satisfy terrestrial ecosystem nutrient demands (Hungate et al., 2003; Wieder et al., 2015). More importantly, enhanced N and P availability is imbalanced (Penuelas et al., 2013), with a potential to shift many ecosystems toward a more P limited status.

With decades of observational studies and multiple lines of evidence, it is now generally agreed that current terrestrial plant growth is often nutrient limited, and these nutrient limitations will be exacerbated under

higher atmospheric CO₂ levels (Hungate et al., 2003; Koerselman & Meuleman, 1996; Wieder et al., 2015; Xia & Wan, 2008). For example, global meta-analyses of N and P fertilization experiments (Elser et al., 2007) revealed widely distributed N and P colimitation on plant productivity in a wide range of terrestrial ecosystems.

Free Air CO₂ Enrichment (FACE) experiments also have provided insights into possible exacerbation of terrestrial nutrient limitation under anticipated higher atmospheric CO₂ concentrations. Under elevated atmospheric CO₂, plants are stimulated to increase tissue construction but require more nutrients to support this higher productivity (Finzi et al., 2007). From a resources supply point of view, a system will shift to a status more limited by other resources when the supply of one resource is continuously enhanced (F S Chapin et al., 1987). Across many FACE experiments, the observed CO₂ fertilization effect on plant growth is sustained for only a few years and then diminishes, because the systems shift to more nutrient limited conditions (Norby et al., 2010; Reich et al., 2006; Reich & Hobbie, 2013).

Although they provide characterization of ecosystem nutrient limitation, empirical experiments cover only a small fraction of global ecosystems, making it difficult to delineate large-scale nutrient limitation patterns. To quantify global impacts of nutrient limitations on the carbon cycle, process-based land models are needed to extrapolate site-level mechanistic understanding to larger scales (Norby et al., 2016). Prevailing Earth System Model (ESM) land models (e.g., those participating in Coupled Model Intercomparison Project Phase 5 [CMIP5; Taylor et al., 2012] and CMIP6 (Eyring et al., 2016)), all consider nitrogen cycles (Gerber et al., 2010; Goll et al., 2012; Koven et al., 2013; Wang et al., 2010; Xu & Prentice, 2008; Yang et al., 2014; Zaehle & Dalmonech, 2011; Zhu & Zhuang, 2013). Some of them also consider the phosphorus cycle (Goll et al., 2012; Wang et al., 2010; Yang et al., 2014). Although these models were built with the concept that nutrient deficiency limits the carbon cycle, large uncertainties stem from how nutrient limitations are implemented (Medlyn et al., 2016; Tang & Riley, 2018; Zaehle et al., 2014).

In this study, we describe the integration of N and P dynamics in the Energy Exascale Earth System Model (E3SM) Land Model version 1 (ELMv1-ECA) and evaluate the model's performance against a wide range of global-scale observations. Compared to its predecessor (i.e., the Community Land Model version 4.5 [CLM4.5]), ELMv1-ECA has several important features, including (1) the equilibrium chemistry approximation (ECA) as a robust method to resolve multiple nutrient (N and P) competition by multiple consumers (plants, microbes, and soil mineral surfaces), (2) leaf-level nutrient effects on photosynthesis, (3) a dynamic allocation scheme that balances concurrent constraints on plants, and (4) explicit representation of leaf and root traits that affect growth and nutrient competitiveness. By comparing our model with baseline versions (CLM4 and CLM4.5), we show an improvement of predictive skill by improving nitrogen constraint and introducing phosphorus constraint on the carbon cycle.

2. Materials and Methods

2.1. E3SM Land Model

The Energy Exascale Earth System Model (E3SM) is a new ESM project sponsored by the U.S. Department of Energy (DOE; Bader et al., 2014) that focuses on addressing critical questions about the global water cycle, biogeochemistry, cryosphere, and their interactions with the climate system. The E3SM land model version zero (ELMv0) originated from the CLM4.5 (CLM4.5-BGC) with vertically resolved soil biogeochemistry and a CENTURY-like soil decomposition cascade (Koven et al., 2013). Both CLM4.5-BGC and ELMv0 represent coupled carbon and nitrogen interactions, and here we describe a new representation of coupled C, N, and P dynamics being integrated in ELM (Figure 1).

2.2. Nutrient Competition in the Plant-Soil System

Plants, soil microbes, and abiotic factors (e.g., mineral surfaces) reside in the same soil media and compete for a wide range of nutrients, including those we focus on here: NH₄⁺, NO₃⁻, and PO₄³⁻. Because these nutrients are usually limited in availability, strong competitive interactions are expected. This section describes the methods ELMv1-ECA uses to represent plant and soil nutrient uptake and competition.

2.2.1. Plant Nutrient Uptake

In ELMv1-ECA, we model plant N and P uptake by explicitly representing several root traits important for nutrient acquisition: (1) root nutrient carrier enzyme kinetics, (2) activation and deactivation of nutrient

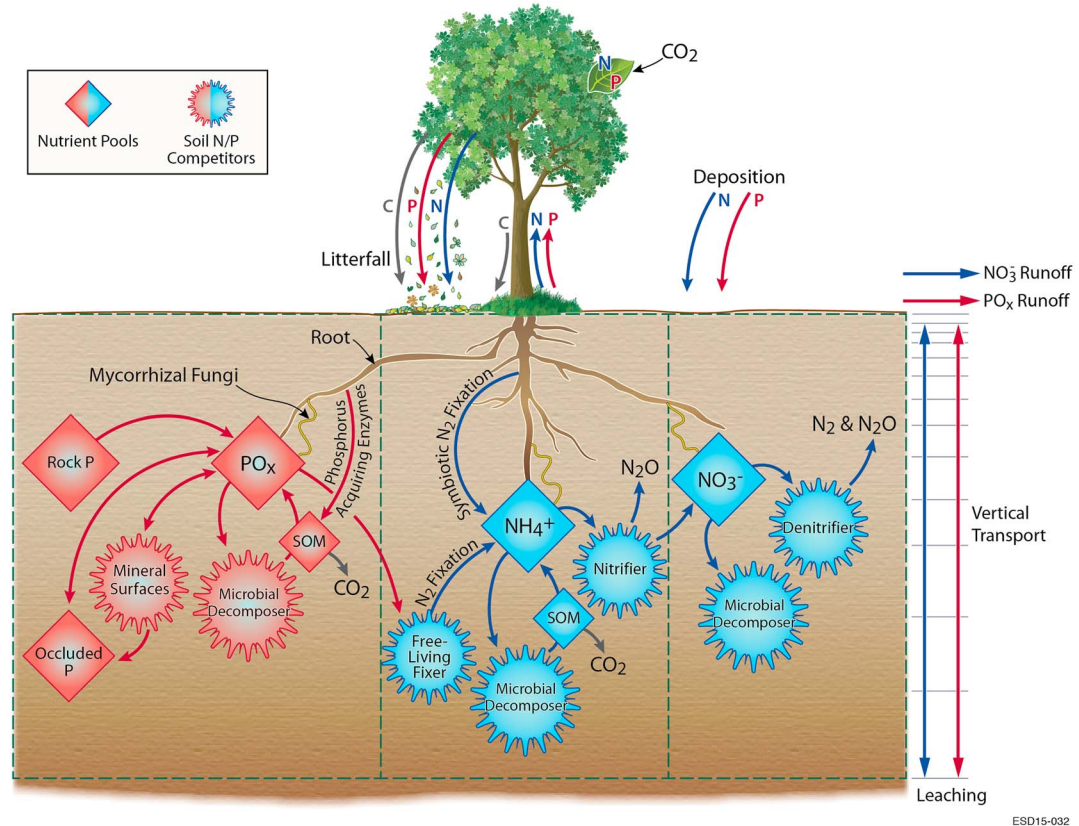


Figure 1. Illustration of Energy Exascale Earth System Model (E3SM) Land Model version 1-equilibrium chemistry approximation (ELMv1-ECA) major features: (1) prognostic leaf N and P content directly coupled to leaf level CO_2 sequestration; (2) multiple-consumer competition network for soil nutrients including NH_4^+ , NO_3^- , and PO_x ; and (3) dynamic carbon allocation for leaf, stem, and root that balance whole plant resources acquisition (e.g., N, P, light, and water). (Free-living N_2 fixation and mycorrhizal fungi are not included in the version applied here).

carrier enzymes controlled by plant nutritional level, (3) direct plant competition with other soil nutrient consumers (e.g., microbes), and (4) nutrient carrier enzyme mediated resource uptake preference (e.g., NH_4^+ versus NO_3^- ; e.g., Zhu et al. 2016, 2017):

$$\text{NF}_{\text{plant}}^{\text{NH}_4} = U_{\max}^{\text{NH}_4} C_{\text{root}} f\left(\text{ECA}_{\text{plant}}^{\text{NH}_4}\right) f(\text{CN}) f(T), \quad (1)$$

$$\text{NF}_{\text{plant}}^{\text{NO}_3} = U_{\max}^{\text{NO}_3} C_{\text{root}} f\left(\text{ECA}_{\text{plant}}^{\text{NO}_3}\right) f(\text{CN}) f(T), \quad (2)$$

$$\text{PF}_{\text{plant}} = U_{\max}^{\text{P}} C_{\text{root}} f\left(\text{ECA}_{\text{plant}}^{\text{P}}\right) f(\text{CP}) f(T), \quad (3)$$

where $U_{\max}^{\text{NH}_4}$, $U_{\max}^{\text{NO}_3}$, and U_{\max}^{P} are maximum nutrient uptake rates per unit fine root biomass at 25°C for NH_4^+ , NO_3^- , and phosphate, respectively (see Table S1 in the supporting information for relevant kinetic parameters); C_{root} is fine root biomass; and $f(\text{ECA})$ accounts for multiple-consumer competition for the same nutrient.

$f(\text{CN})$ and $f(\text{CP})$ account for the regulation of plant nutritional level on nutrient carrier enzyme activity. When leaf level C:N or C:P ratio (CN^{leaf} and CP^{leaf}) is smaller than its baseline value ($\text{CN}_{\text{baseline}}^{\text{leaf}}$, $\text{CP}_{\text{baseline}}^{\text{leaf}}$), only a portion of the nutrient carrier enzymes are activated ($f(\text{CN})$ and $f(\text{CP}) < 1$), thereby down-regulating the plant nutrient uptake rate. This representation therefore follows the idea that plants maintain a healthy level of internal nutrient stocks to buttress against environmental nutrient supply fluctuations. $f(T)$ is a vertically resolved temperature Q_{10} scalar that accounts for the variation of enzyme activity due to the deviation of soil temperature (T_{soil}) from a reference temperature (T_{ref}).

$$f(\text{CN}) = \min\left(\frac{\text{CN}^{\text{leaf}} - \text{CN}_{\min}^{\text{leaf}}}{\text{CN}_{\text{baseline}}^{\text{leaf}} - \text{CN}_{\min}^{\text{leaf}}}, 1\right), \quad (4)$$

$$f(\text{CP}) = \min\left(\frac{\text{CP}^{\text{leaf}} - \text{CP}_{\min}^{\text{leaf}}}{\text{CP}_{\text{baseline}}^{\text{leaf}} - \text{CP}_{\min}^{\text{leaf}}}, 1\right), \quad (5)$$

$$f(T) = Q10^{\frac{T_{\text{soil}} - T_{\text{ref}}}{10}}. \quad (6)$$

As an example ECA term, $f(\text{ECA}_{\text{plant}}^{\text{NH}_4})$ represents plant competition for soil NH_4^+ (see Method S1 in the supporting information for full description of all ECA terms):

$$f(\text{ECA}_{\text{plant}}^{\text{NH}_4}) = \frac{[E_N^{\text{plant}}]}{K_M^{\text{plant,NH}_4} \left(1 + \frac{[\text{NH}_4]}{K_M^{\text{plant,NH}_4}}^{(1)} + \frac{[\text{NO}_3]}{K_M^{\text{plant,NO}_3}}^{(2)} + \frac{[E_N^{\text{plant}}]}{K_M^{\text{plant,NH}_4}}^{(3)} + \frac{[E_N^{\text{mic}}]}{K_M^{\text{mic,NH}_4}}^{(4)} + \frac{[E_N^{\text{nit}}]}{K_M^{\text{nit,NH}_4}}^{(5)} \right)}, \quad (7)$$

where $[E]$ and K_M denote enzyme abundance and half saturation constants (i.e., substrate-enzyme affinity), respectively. Superscripts and subscripts of K_M refer to consumers and substrates, respectively. These equations account for the effect of (1) multiple substrates (e.g., NH_4^+ and NO_3^-) sharing one consumer, which inhibits the effective binding between any specific substrate and the consumer (terms ⁽¹⁾ and ⁽²⁾ in equation (2)) and (2) multiple consumers (e.g., plants, decomposing microbes, and nitrifiers) sharing one substrate (e.g., NH_4^+), which lowers the probability of effective binding between any consumer and NH_4^+ (terms ⁽³⁾, ⁽⁴⁾, and ⁽⁵⁾ in equation (7)).

2.2.2. Soil Nutrient Uptake

In the century-like decomposition cascade, there are seven litter and soil organic matter pools with different turnover times and stoichiometries: (1) coarse woody debris; (2) metabolic, cellulose, and lignin litter (litter 1-3); and (3) fast, medium, and slow mineral soil pools (SOM 1-3; Koven et al., 2013). Our approach assumes that soil microbes immobilize inorganic N and P to maintain their C:N:P stoichiometric balance during decomposition:

$$\text{NF}_{\text{soil},i \rightarrow j}^{\text{pot}} = f_{ij} k_j C_j f(\theta) f(T) \max\left(\frac{g_i}{\text{CN}_j} - \frac{1}{\text{CN}_i}, 0\right), \quad (8)$$

$$\text{PF}_{\text{soil},i \rightarrow j}^{\text{pot}} = f_{ij} k_j C_j f(\theta) f(T) \max\left(\frac{g_i}{\text{CP}_j} - \frac{1}{\text{CP}_i}, 0\right), \quad (9)$$

where $\text{NF}_{\text{soil},i \rightarrow j}^{\text{pot}}$ and $\text{PF}_{\text{soil},i \rightarrow j}^{\text{pot}}$ are potential mineral N and P immobilization rates when an upstream soil organic matter pool i is decomposed. A fraction of the decomposed organic matter remains in the soil (g_i or carbon use efficiency) and is incorporated into the j th downstream pool (f_{ij}). k_j and C_j are turnover rate and organic carbon stocks of the j th pool, respectively, and $f(\theta)$ and $f(T)$ are soil temperature and moisture scaling factors, respectively.

Soil nitrifiers consume NH_4^+ ($\text{NF}_{\text{nit}}^{\text{pot}}$) to produce NO_3^- under aerobic conditions. Following the approach in ELMv0, the potential nitrification rate is modeled as a linear function of NH_4^+ substrate concentration:

$$\text{NF}_{\text{nit}}^{\text{pot}} = [\text{NH}_4^+] k_{\text{nit}} f(\theta) f(T) (1 - f^{\text{anox}}), \quad (10)$$

where k_{nit} is the maximum fraction of substrate to be consumed, $f(\theta)$, $f(T)$, are f^{anox} are soil moisture, temperature, and oxygen scalars, respectively.

Soil denitrifiers consume NO_3^- to produce N_2 and N_2O under anaerobic conditions (which can be either in anaerobic bulk soil layers or the anaerobic fraction of aerobic bulk soil layers; f^{anox}). The potential denitrification rate can be limited by carbon (energy) or NO_3^- substrate supply:

$$\text{NF}_{\text{den}}^{\text{pot}} = \min(f(\text{decomp}), f([\text{NO}_3^+])) f^{\text{anox}}, \quad (11)$$

where $f(\text{decomp})$ and $f([\text{NO}_3^+])$ are carbon limited and NO_3^- limited denitrification rates (Del Grosso et al., 2000).

In contrast to approaches that assume mineral surface adsorbed P is in equilibrium with solution phosphate after plant and soil microbe P demands have been satisfied (Yang et al., 2014), in ELMv1-ECA the potential P adsorption rate is calculated as the time derivative of the Langmuir isotherm equation (Wang et al., 2010).

$$PF_{\text{surf}}^{\text{pot}} = \frac{U_P^{\text{surf}} \cdot K_P^{\text{surf}}}{(K_P^{\text{surf}} + [\text{PO}_x])^2} \frac{d[\text{PO}_x]}{dt}. \quad (12)$$

where U_P^{surf} and K_P^{surf} are Langmuir isotherm parameters representing the maximum adsorption potential and half saturation constant, respectively, and $[\text{PO}_x]$ represents solution P (i.e., the sum of PO_4^{3-} , HPO_4^{2-} , and H_2PO_4^-).

2.2.3. Nutrient Competition

As soil nutrient availability decreases, competitive stresses increase, particularly when the potential nutrient demands by all nutrient consumers exceed the supply in a given time step. The partitioning of limited nutrients between consumers affects their functioning. Consequently, model predictability of carbon-nutrient dynamics is sensitive to the underlying model hypotheses regarding nutrient competition. In ELMv1-ECA we adopted a multiple-consumer-multiple-substrate competition network based on the ECA theory (Tang & Riley, 2013; Zhu et al., 2016; Zhu et al., 2017; Zhu, Riley, et al., 2016). The ECA competition theory represents (1) nutrient uptake mediated by nutrient carrier enzymes, (2) binding of a nutrient substrate to a specific enzyme prevents it from binding to other enzymes, and (3) rates and affinities of consumers for the various substrates.

In the ECA approach, potential immobilization ($NF_{\text{soil},i \rightarrow j}$, $PF_{\text{soil},i \rightarrow j}$), nitrification (NF_{nit}), denitrification (NF_{den}), and mineral sorption rates (PF_{surf} ; equations (13)-(17)) are modified by an ECA term that accounts for (1) multiple consumers competing for a single nutrient species and (2) a single consumer competing for multiple nutrient species (see Method S1 for description of the ECA terms):

$$NF_{\text{soil},i \rightarrow j} = NF_{\text{soil},i \rightarrow j}^{\text{pot}} f(\text{ECA}_{\text{dec,N}}), \quad (13)$$

$$PF_{\text{soil},i \rightarrow j} = PF_{\text{soil},i \rightarrow j}^{\text{pot}} f(\text{ECA}_{\text{dec,P}}), \quad (14)$$

$$NF_{\text{nit}} = NF_{\text{nit}}^{\text{pot}} f(\text{ECA}_{\text{nit}}), \quad (15)$$

$$NF_{\text{den}} = NF_{\text{den}}^{\text{pot}} f(\text{ECA}_{\text{den}}), \quad (16)$$

$$PF_{\text{surf}} = PF_{\text{surf}}^{\text{pot}} f(\text{ECA}_{\text{surf}}). \quad (17)$$

2.3. N and P Impacts on Carbon Dynamics

2.3.1. Plant Carbon Assimilation

ELMv1-ECA represents the photosynthesis rate as a function of leaf N (Inc: gN/m² leaf area) and leaf P (Ipc: gP/m² leaf area) contents, which are commonly measured leaf properties, and their fundamental controls on plant photosynthesis rates are widely supported by observations (Kattge et al., 2009; Reich et al., 2009) and theory (Gardesröm & Wigge, 1988; Woodrow & Berry, 1988). ELMv1-ECA adopts the following relationships to model $VC_{\max 25}$ (maximum carboxylation rate at 25 °C), and $J_{\max 25}$ (maximum electron transport rates at 25 °C) as functions of N_L and P_L (Walker et al., 2014):

$$\ln(VC_{\max 25}) = a \ln(N_L) + b \ln(P_L) + c \ln(N_L) \ln(P_L), \quad (18)$$

$$\ln(J_{\max 25}) = d \ln(VC_{\max 25}) + e \ln(P_L), \quad (19)$$

where a , b , c , d , and e are regression coefficients estimated from a photosynthesis data set covering more than 300 plant species (Walker et al., 2014). These two relationships allow ELMv1-ECA to dynamically represent direct nutrient constraints on photosynthesis.

2.3.2. Carbon Allocation

New photosynthates are allocated to different plant organs to satisfy the plant's metabolic demands. To account for nutrient regulation of carbon allocation, we apply a general allocation framework (Friedlingstein et al., 1999; Sharpe & Rykiel, 1991) that considers multiple resource availability:

$$f \propto \frac{\sum x}{\sum x + \sum y} \quad (20)$$

where f is the fraction of NPP allocated to a certain plant compartment (e.g., stem, j) and x and y represent resource availabilities. Increasing resource availability x_i will increase allocation fraction, and conversely, increasing resource availability y_j will decrease allocation fraction. Currently, the model considers four types of resources: carbon (C), nitrogen (N), phosphorus (P), and water (W; see Method S2 for calculation of resource availability).

2.3.3. Prognostic Plant Stoichiometry

To account for plants' plasticity in assimilating and using nutrients, ELMv1-ECA allows C:N:P stoichiometry to be flexible, varying around a baseline value and prognostically determined by leaf level carbon fixation versus root nutrient uptake. The baseline C:N:P ratio is derived from the TRY database (leaf C:N:P; Kattge et al., 2009) and a recent synthesis of global fine root, sapwood, and heartwood C:N:P including more than 6,000 plant species (see Table S2 for plant functional type-specific C:N:P stoichiometry). The model stoichiometric baseline and natural variability are based on stoichiometric mean and standard deviation in the data set (Table S2). Root nutrient uptake is regulated (equations (4) and (5)) so that plant tissue nutritional levels are maintained within the range of this observed natural variability, which we estimate to be 40% of the baseline value. If N or P supply were highly limited, plant biomass construction would be reduced and the excess nonstructural carbon would be stored within the plant.

2.4. Model Configuration and Benchmarking

Following the simulation protocol of CLM (Oleson et al., 2013), ELMv1-ECA was first spun up for 1,000 years with accelerated soil decomposition (Koven et al., 2013) followed by a 200-year regular spin up with regular soil decomposition to reach a steady state carbon cycle. Soil phosphorus pools were initialized from observations (Yang et al., 2013) at the beginning of the regular spin-up. The spin-up simulations were forced with repeated meteorology and constant atmospheric CO₂ mole fraction (285 ppm). The model was then run in a transient simulation from 1850 to 2010 with Global Soil Wetness Project (GSWP) reanalysis forcing (Dirmeyer et al., 2006), transient CO₂ concentrations, N deposition (Lamarque et al., 2005), and P deposition (Mahowald et al., 2008). Model simulations were performed at a 1.9° latitude by 2.5° longitude resolution.

Simultaneously evaluating global land model carbon pool and flux predictions is complex (Luo et al., 2012), particularly since improving one aspect of model performance can often lead to degradation in others. To address this problem, the ILAMBv2.2 (International Land Model Benchmarking; Collier et al., 2016; Hoffman et al., 2017) package was designed to evaluate land models across a wide range of observational constraints, including ecosystem states, fluxes, and functional responses. The full ILAMBv2 package includes model evaluations against observations of the carbon cycle, water cycle, energy cycle, and climate forcing at in situ, regional, and global scales. We focus here on the global patterns of carbon cycle-related benchmark metrics, including (1) gross primary productivity and total ecosystem respiration, (2) leaf area index (LAI), (3) soil carbon stock, (4) aboveground live biomass, and (5) evapotranspiration (ET). The global patterns of gross primary productivity (GPP) is upscaled from FLUXNET in situ observations (Baldocchi, 2003) using a model tree ensemble (MTE) technique (Beer et al., 2010). FLUXNET-MTE total ecosystem respiration is derived from nighttime measurements extrapolated to daytime based on calculated temperature sensitivities (Reichstein et al., 2005). The global ET benchmark is derived from the annual average of the GLEAM estimated sum of canopy and soil evaporation, transpiration, bare soil evaporation, and sublimation using multiple satellite sensor data (Miralles et al., 2011). The aboveground living biomass benchmark is based on more than 4,000 inventory plots and extrapolated to large-scale with high-resolution remote sensing imagery (Saatchi et al., 2011). We include two independent benchmarks for the top 1-m soil carbon stock: (1) NCSCD (The Northern Circumpolar Soil Carbon Database) for the northern pan-Arctic region (Hugelius et al., 2013) and (2) HWSD (Harmonized World Soil Database) for the globe (Hiederer & Köchy, 2011). We also benchmark CLM4.0-CN (Thornton et al., 2007) and CLM4.5-BGC (Koven et al., 2013) to show improvements of ELMv1-ECA modeling skills. Compared with ELMv1-ECA, CLM4.0 and CLM4.5 both consider carbon and nitrogen cycles but not phosphorus. Further, CLM4.0 and CLM4.5 employed a relative demand hypothesis for nutrient competition among plants, microbial decomposers, nitrifiers, and denitrifiers, in which different nutrient consumers take up soil available nutrients based on their gross demand rather than actual capability. A major improvement of CLM4.5 over CLM4.0 was to

include a vertically resolved CENTURY type soil decomposition module (Koven et al., 2013). In conducting simulations, all three models used a similar spin-up strategy (accelerated spin-up and regular spin-up), land use time series, definition of plant functional type, and global distribution of plant function types. CLM4.0 and CLM4.5 used CRUNEP climate forcing, while ELMv1-ECA used GSWP3 climate forcing.

3. Results and Discussion

3.1. Global Carbon fluxes

We first evaluate the models using the spatial distribution of long-term GPP annual means (1982–2008; Figure 2). The largest model GPP biases are in Northern American boreal forest ecosystems and lowland tropical ecosystems (overestimation) and Northern Eurasia boreal forest ecosystems (underestimation), although the globally integrated bias has been reduced compared with CLM4.0-CN and is similar to that of CLM4.5-BGC (Table 1). The spatial pattern and bias of modeled GPP have been largely reduced compared with the baseline models, resulting in ELMv1-ECA GPP having the highest score (0.78) for this benchmark (Table 1).

Since photosynthesis (GPP) synthesizes organic carbon using CO₂ via metabolic reactions catalyzed by the temperature sensitive Rubisco enzyme, GPP is closely related to water availability, temperature, and plant ET. The observed relationships between those factors and GPP provide useful benchmarks for GPP modeling (Figure 3). As ET, temperature, and precipitation increase, observed (i.e., FLUXNET-MTE) GPP (green line) first increases, then plateaus, and finally declines due to environmental stresses (e.g., high temperature). CLM4.0-CN overpredicts GPP when ET and precipitation are high, while CLM4.5-BGC and ELMv1-ECA are comparable and more consistent with the benchmark. ELMv1-ECA best captures the observed relationship between GPP and ET, particularly when ET ranges from 2 to 4 mm/day. The three models also share some common bias features. Consistently, maximal GPP bias from all three models were around 20°C, which highlight the model deficiency in representing photosynthesis in subtropical ecosystems and an urgent need for future development and improvement for this particular ecosystem.

In terms of total ecosystem respiration (R_{eco}), all three models shared a similar error spatial structure. That is, R_{eco} is overestimated in most of the tropical rainforest and northern high-latitude ecosystems (Figure 4). However, the integrated error in ELMv1-ECA was much smaller than that in CLM4.5-BGC and CLM4.0-CN, with their global root-mean-square error scores being 0.68, 0.62, and 0.54, respectively (Table 1). We note that R_{eco} and GPP from the FLUXNET-MTE product are not independent, because each was derived from the observed net ecosystem exchange by assuming that respiration is temperature dependent and that nighttime temperature sensitivity is maintained over the diurnal cycle.

Two available benchmarks for net biome production were used in this study, including the Global Carbon Project (GCP) estimate (Le Quéré et al., 2016) and Hoffman et al. (2014). We found that ELMv1-ECA agreed better with the GCP net biome production estimates than with the Hoffman et al., 2014 estimates, over the time period when ELMv1-ECA, GCP, and Hoffman et al. (2014) estimates are all available and evaluated in terms of capturing the interannual variability (Figure S1a in the supporting information) and the overall probability density distributions (Figure S1b).

3.2. Leaf Area Index

LAI, the single-sided leaf area per unit ground area, is a critical vegetation property that affects canopy-scale photosynthesis. The ILAMB LAI global benchmark is derived from the Moderate Resolution Imaging Spectroradiometer (MODIS) LAI collection 5 product (MCD15A3; Figure 5). Except for the Arctic and African semiarid regions, all three models tend to overestimate LAI. This overestimation could be due to model parameter or structural biases and/or MODIS LAI algorithm bias. Previous efforts found that although MCD15A3 has been significantly improved compared with the collection 4 product, it still underestimated maximum LAI for high LAI systems, such as mature forests (De Kauwe et al., 2011). Model-data LAI discrepancy is smallest in ELMv1-ECA, and largest in CLM4.0-CN (Figure 5). Global mean LAI bias of ELMv1-ECA ($1.9 \text{ m}^2/\text{m}^2$) is ~30% lower than CLM4.0-CN and CLM4.5-BGC (2.2 and $2.3 \text{ m}^2/\text{m}^2$, respectively; Table 1). Although the gridcell level bias of ELMv1-ECA is much lower compared to the other two models, ELMv1-ECA still overestimates LAI over a large fraction of the land surface (e.g., tropics), which warrants further investigation and improvement of model performance and benchmark data.

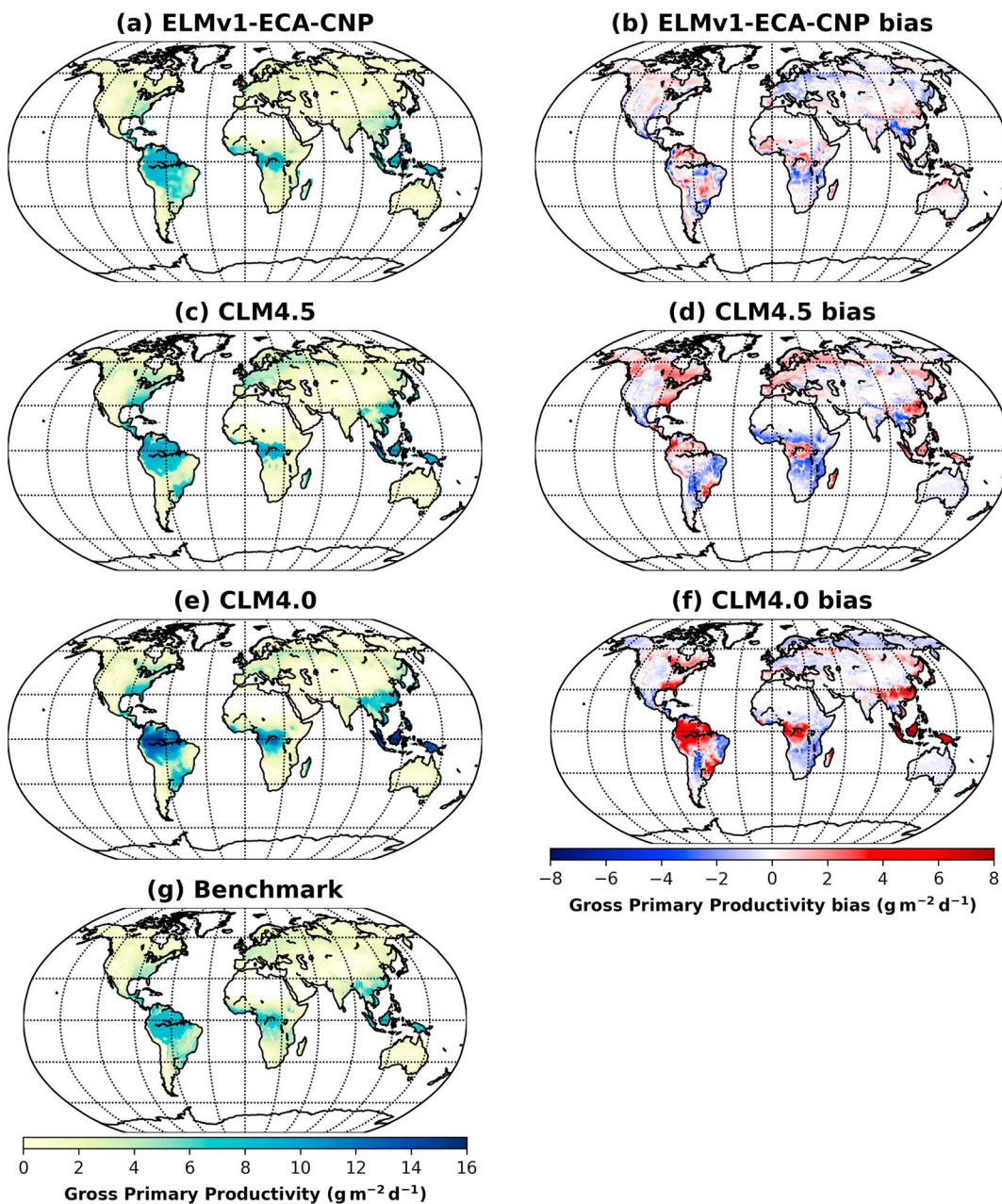


Figure 2. Global patterns of mean gross primary productivity and bias (model-benchmark) using the International Land Model Benchmarking (ILAMB) package. Energy Exascale Earth System Model (E3SM) Land Model version 1-equilibrium chemistry approximation (ELMv1-ECA) and Community Land Model version 4.5(CLM4.5) performed generally better than CLM4.0, particularly over the tropical forest region.

The observed relationship between LAI and precipitation (Figure 6, green line) indicates that lowland tropical regions (precipitation over 7 mm/day) had the highest potential of developing large LAI. ELMv1-ECA LAI in the lowland tropics is about $6 \text{ m}^2/\text{m}^2$ (Figures 5 and 6), while CLM4.0-CN and CLM4.5-BGC are 8 and $10 \text{ m}^2/\text{m}^2$, respectively. Given that the satellite-derived maximum mean LAI in tropical regions is probably substantially underestimated because of cloud contamination (e.g., at a site in Tapajos Brazil, MCD15A3 indicates LAI of $4 \text{ m}^2/\text{m}^2$, which is $\sim 2 \text{ m}^2/\text{m}^2$ lower than ground camera-based LAI measurements; Wu et al., 2016) and data algorithm saturation (Heiskanen et al., 2012), an estimate of $6\text{-}7 \text{ m}^2/\text{m}^2$ for tropical forest LAI is expected, which is consistent with the ELMv1-ECA estimate.

Table 1ILAMB Benchmark Scores for Gross Primary Productivity (GPP), Total Ecosystem Respiration (R_{eco}), Leaf Area Index (LAI), and Evapotranspiration (ET)

	Mean	RMSE	Bias score	RMSE score	Seasonal cycle score	Spatial distribution score	Overall score
GPP	[Pg/year]	[Pg/year]					
Benchmark	113						
ELMv1-ECA	126	55	0.80	0.70	0.79	0.94	0.78
CLM4.5-BGC	127	68	0.73	0.65	0.79	0.92	0.75
CLM4.0-CN	140	76	0.66	0.60	0.79	0.79	0.67
R_{eco}	[Pg/year]	[Pg/year]					
Benchmark	90						
ELMv1-ECA	120	47	0.79	0.68	0.84	0.89	0.78
CLM4.5-BGC	122	61	0.72	0.62	0.85	0.83	0.73
CLM4.0-CN	136	74	0.65	0.54	0.81	0.65	0.64
LAI	[m ² /m ²]	[m ² /m ²]					
Benchmark	1.3						
ELMv1-ECA	1.9	1.0	0.64	0.55	0.64	0.81	0.64
CLM4.5-BGC	2.3	1.4	0.51	0.45	0.62	0.56	0.52
CLM4.0-CN	2.2	1.3	0.52	0.47	0.66	0.56	0.54
ET	[mm/day]	[mm/day]					
Benchmark	1.2						
ELMv1-ECA	1.2	0.46	0.84	0.74	0.81	0.94	0.81
CLM4.5-BGC	1.3	0.57	0.80	0.68	0.83	0.92	0.78
CLM4.0-CN	1.4	0.66	0.73	0.64	0.82	0.86	0.74

Note. The bold numbers represent the best model.

Abbreviations: CLM4.5-BGC, Community Land Model version 4.5 BGC; ELMv1-ECA, Energy Exascale Earth System Model (E3SM) Land Model version 1-equilibrium chemistry approximation; ILAMB, International Land Model Benchmarking; RMSE, root-mean-square error.

3.3. Evapotranspiration

ET is tightly coupled to leaf level carbon dynamics. For example, in ELMv1 a better representation of photosynthesis rate (A_n) will potentially improve the estimate of stomatal resistance (r_s), based on the Ball-Berry conductance model ($\frac{1}{r_s} = m \frac{A_n}{C_s/P_{atm}} h_s + b\beta_t$) and thus the calculation of ET. The observed annual ET is higher in the tropics and lower in the boreal region (Figure 7). Although all three models capture the general observed spatial distribution, CLM4.0-CN and CLM4.5-BGC substantially overpredict ET in the tropics; this bias is significantly lower in ELMv1-ECA (Figure 7). All models tend to underestimate ET in the northern high latitudes, although the absolute biases are smaller than in the tropics. The global mean square error of ELMv1-ECA ET is 0.46 mm/day, significantly less than that of CLM4.5-BGC (0.57 mm/day) and CLM4.0-CN (0.66 mm/day). Further, the spatial distribution of ELMv1-ECA ET better matched observations than did CLM4.0-CN and CLM4.5-BGC (Table 1).

For precipitation between 6 and 14 mm/day (~2,000–5,000 mm/year), CLM4.0-CN predicts relatively higher ET compared to observations (Figure 8). CLM4.5-BGC and ELMv1-ECA both generally follow the observed

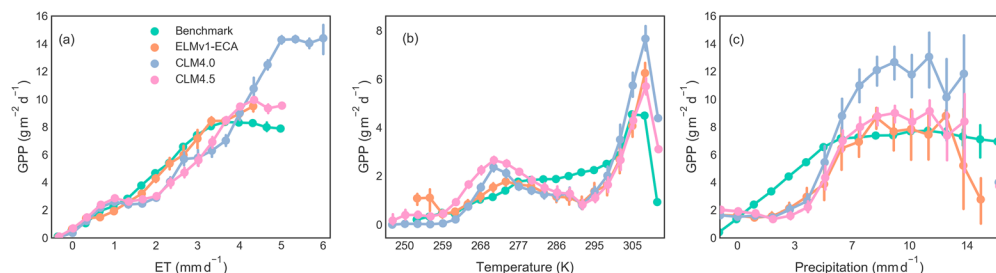


Figure 3. Empirical relationship between Energy Exascale Earth System Model (E3SM) Land Model version 1-equilibrium chemistry approximation (ELMv1-ECA), Community Land Model version 4.0 CN (CLM4.0-CN), and CLM4.5-BGC modeled gross primary productivity (GPP) and (a) evapotranspiration (ET), air temperature, and (c) precipitation. The error bar represents the variation of GPP within each evapotranspiration (ET), temperature, or precipitation bins, which implied a relatively large variation of GPP in all models when a precipitation larger than 7 mm/day.

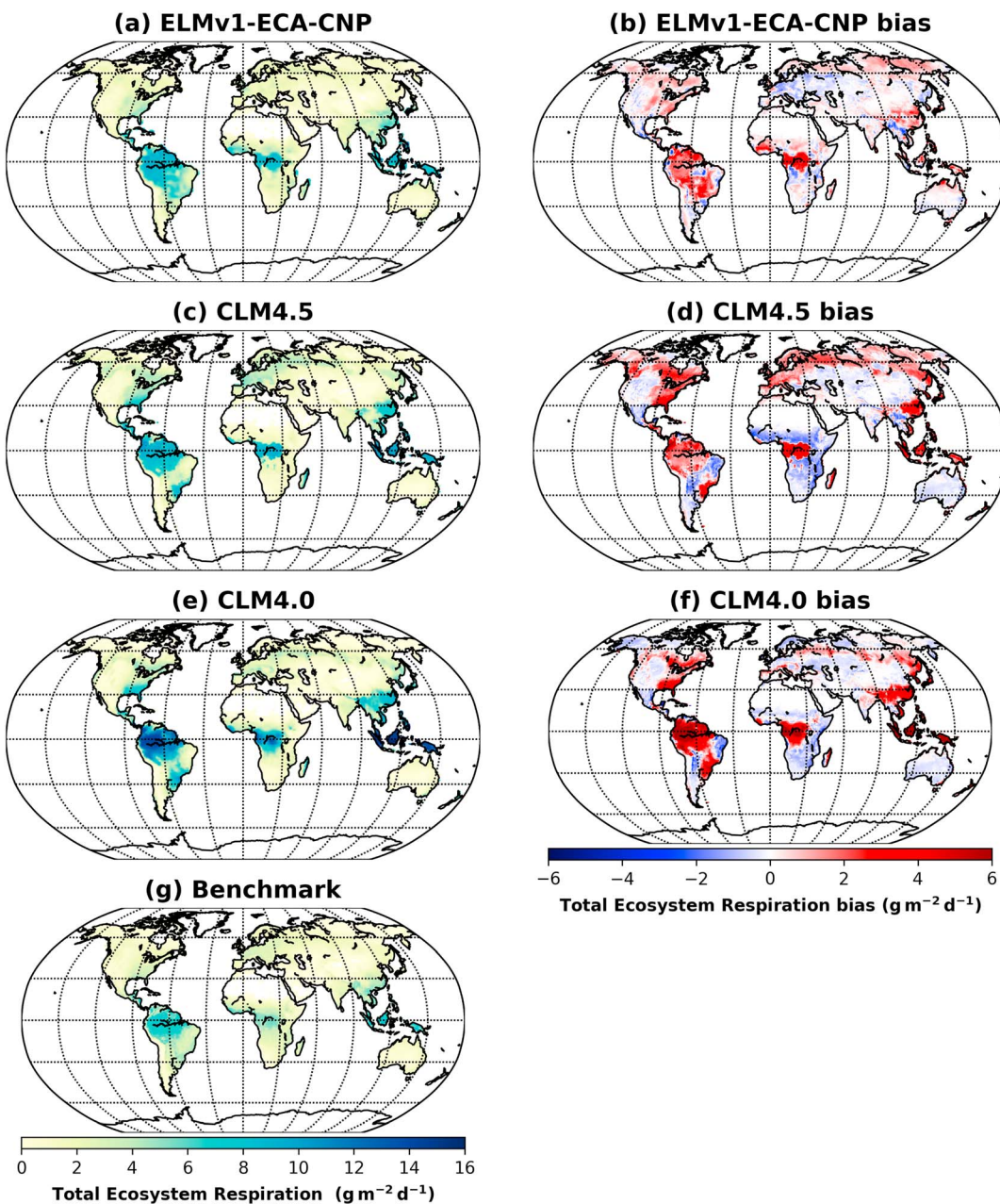


Figure 4. Global patterns of total ecosystem respiration and bias (model-benchmark). Biases were relatively larger over tropical and high latitude ecosystems in Community Land Model version 4.0 (CLM4.0) compared with midlatitude regions. The tropical model bias was largely reduced in CLM4.5, but not over the high latitudes. In Energy Exascale Earth System Model (E3SM) Land Model version 1-equilibrium chemistry approximation (ELMv1-ECA) both tropical and high-latitude ecosystems were largely improved, compared with CLM4.0.

pattern, with ELMv1-ECA having an overall lower bias. However, under low annual precipitation (<6 mm/day), all three models underpredict observed ET. The observed relationship between ET and surface air temperature is well captured by all three models (Figure 8). ET initially increases as temperature increases due to higher evaporative energy but declines at very high temperatures, due to the limitation from other factors (e.g., water availability in tropical drylands) rather than temperature.

3.4. Global Carbon Pools

Our benchmark of global carbon pools here focuses on aboveground living biomass and total soil carbon stock to 1-m depth. Highest aboveground biomass (~20 kg C/m²) was observed in the lowland tropics

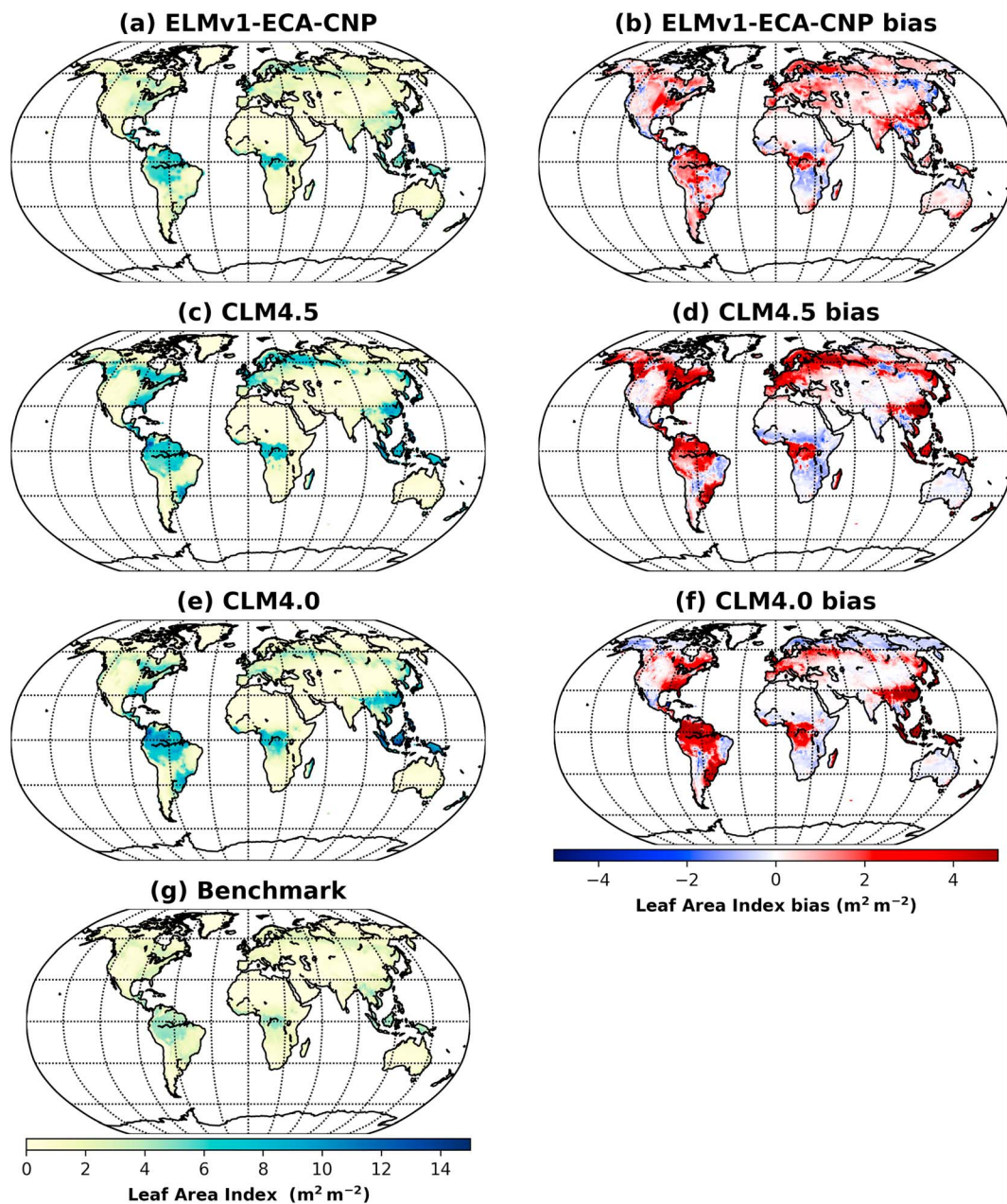


Figure 5. Global patterns of mean leaf area index (LAI) and bias (model-benchmark). Spatial patterns and magnitudes of LAI bias were similar in both Community Land Model version 4.0 (CLM4.0) and CLM4.5 models. Energy Exascale Earth System Model (E3SM) Land Model version 1-equilibrium chemistry approximation (ELMv1-ECA) still overestimated LAI over a large fraction of the globe, but the magnitude of the bias was generally smaller than in CLM4.0 and CLM4.5.

(Figure 9). CLM4.0-CN and CLM4.5-BGC predicted the highest biomass density in the lowland tropics, and their predictions are highly biased (biomass bias of about 50 and 30 kg C/m², respectively). ELMv1-ECA slightly overestimated lowland tropical biomass (Figure 9 and Table 2).

ELMv1-ECA matched both NCSCD and HWSD data sets much better than did CLM4.0-CN or CLM4.5-BGC (Table 3). NCSCD and HWSD are two independent, and often inconsistent, observational benchmarks that may complicate model benchmarking. This problem raises the challenging question of how to harmonize different observational data sets when benchmarking models. It is also important to mention that SoilGrid1km (Hengl et al., 2014) is a third well-known global carbon stock database not yet included in

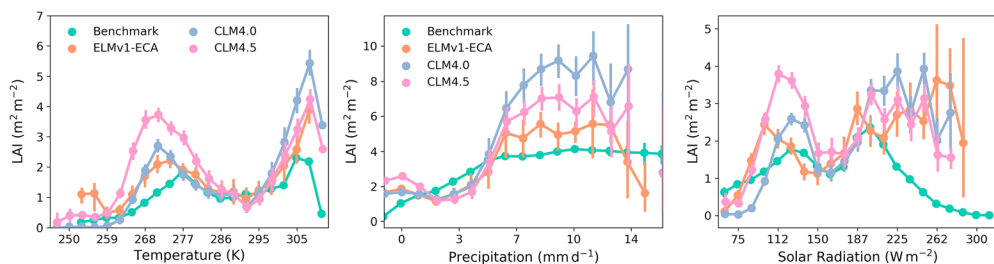


Figure 6. Empirical relationship between leaf area index (LAI) and precipitation. The error bars represent the variation of LAI rather than the uncertainty. LAI was relatively stable in benchmark data set with little variation across different precipitation regimes. However, all three models predicted large variation of LAI when precipitation increased from 6 to 14 mm/day. The model-data biases were also prominent within such precipitation range.

ILAMB, and it differs substantially from both NCSCD and HWSD. Currently, ILAMB weights the NCSCD (45%) and HWSD (55%) metrics to produce an overall score (Collier et al., 2018).

We also evaluated the effects of modeled P cycle and dynamic allocation to modeled carbon pools (living biomass versus soil carbon stock). ELMv1-ECA with an imposed fixed carbon allocation scheme slightly improved LAI estimates but biased all other variables (Figure 10). In particular, using fixed carbon allocation degraded estimates of biomass and SOC. We also note that excluding the P cycle mostly biased the estimates of carbon fluxes, such as GPP and R_{eco} , but with small effects on biomass and SOC. Overall, ELMv1-ECA showed very good ILAMB scores (greenish color in variable z-score panel of Figure S2) in almost all carbon cycle metrics. For water cycle metrics, ELMv1-ECA performed better in ET and latent heat while did worse in terrestrial water storage than CLM4.0 or CLM4.5. For the energy cycle metrics, ELMv1-ECA tended to perform relatively worse in simulating upward shortwave and longwave radiation fluxes and consequently albedo. For the climate forcing metrics, CRUNCEP and GSWP3 were generally similar (variable score panel of Figure S2), although GSWP3 was sometime better than CRUNCEP (variable z-score panel of Figure 3). In summary, ELMv1-ECA performed significantly better than CLM4.0 and CLM4.5 in most of the available metrics including carbon, water, and energy cycles.

3.5. Nutrient Cycle Evaluation

Compared to metrics for the carbon cycle, global-scale gridded benchmarks for nitrogen and phosphorus cycles are less available. In this study, we used nutrient fluxes of NO_3^- leaching and N_2O gases loss (Houlton et al., 2015; Sinha et al., 2017; Zhu & Riley, 2015) to assess the nitrogen loss pathways of ELMv1-ECA. Using soil ¹⁵N tracer information, the fraction of gaseous (N_2O) versus total N ($\text{N}_2\text{O} + \text{NO}_3^-$ leaching) losses (f_{denit} ; Figure 11) was inferred based on different ¹⁵N fractionation effects (Houlton et al., 2015). The latitudinal distribution of observationally-inferred f_{denit} indicates that higher proportions of total N losses occur as gas in the tropics, and this proportion gradually declines toward colder ecosystems. Both CLM4.0 and CLM4.5 failed in simulating this spatial distribution of f_{denit} (Houlton et al., 2015), while ELMv1-ECA generally captured this latitudinal trend. For the phosphorus cycle, which also lacks a global-scale benchmark, we adopt the idea of phosphorus limitation from the leaf C:N:P stoichiometry perspective based on Wang et al. (2010) and developed a latitudinal distribution of P limitation (Figures 11b and S3). This metric is defined by leaf level relative abundance of nitrogen and phosphorus. ELMv1-ECA predictions indicate that ~60% of tropical ecosystems are more phosphorus limited (rather than N limited) and P limitation is alleviated over temperate ecosystems. Across the southern midlatitude ecosystems, P limitation indicates that these low-temperature systems are inefficient in recycling soil phosphorus although the observed total phosphorus content in high latitude soils (slightly weathered) is much higher than in tropical soils (strongly weathered; Yang et al., 2013). This modeled P limitation distribution is consistent with current understanding of the relationship between plant carbon and soil nutrient cycles at a global scale (Houlton et al., 2008; Walker et al., 2014; Wang et al., 2010).

We evaluated the spatial distribution of leaf nutrient concentrations and leaf to fine root biomass ratios, in spite of a lack of global-scale direct measurements, because they represent important aspect of the model in terms of carbon-nutrient coupling. The modeled long-term averaged leaf C to N ratio was highest in

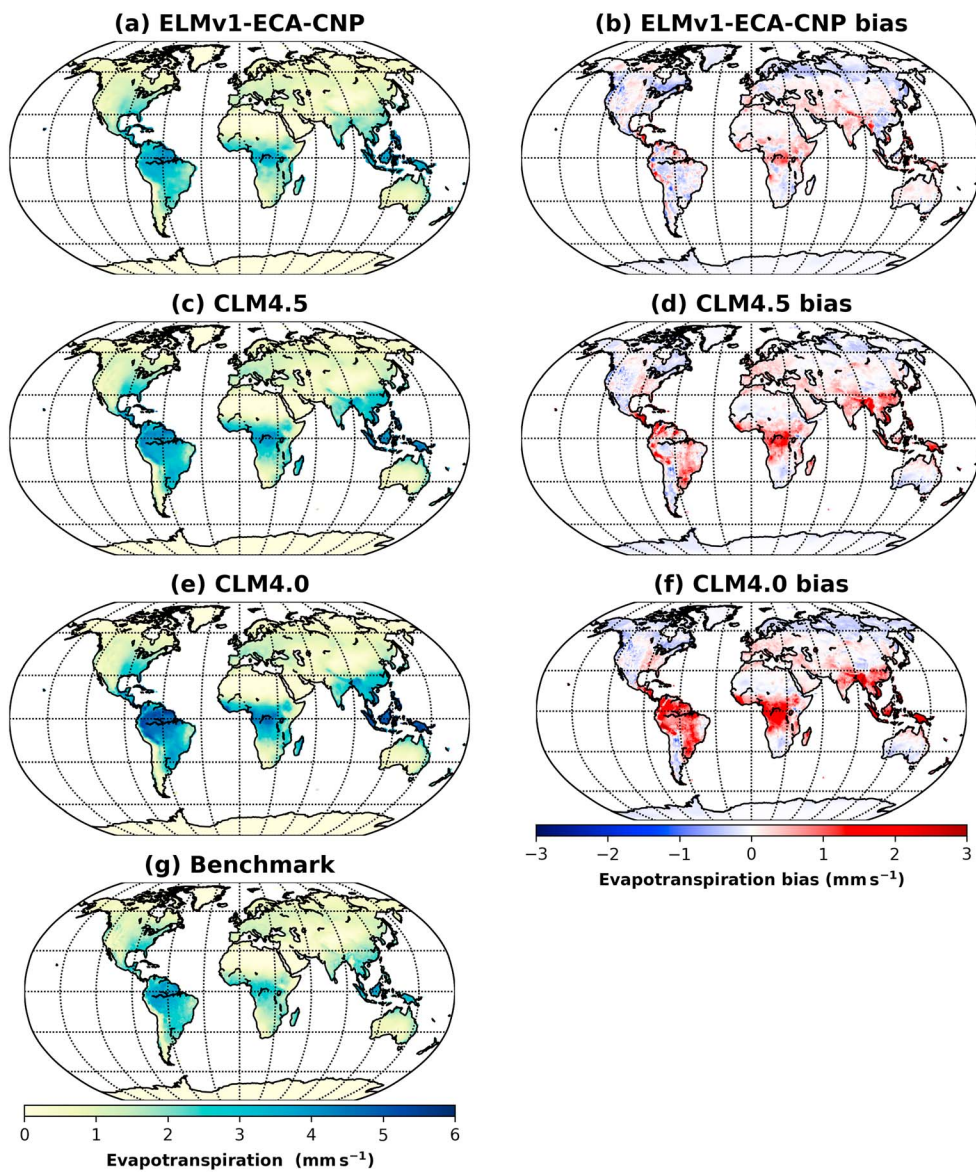


Figure 7. Global patterns of mean evapotranspiration (ET) and bias (model-benchmark). Energy Exascale Earth System Model (E3SM) Land Model version 1-equilibrium chemistry approximation (ELMv1-ECA) and Community Land Model version 4.0 (CLM4.0) overestimated ET over the tropics and underestimated ET over the boreal regions, although the magnitude of ELMv1-ECA bias over the tropics is much less. However, CLM4.5 overestimated ET over both tropical regions and most of the boreal regions.

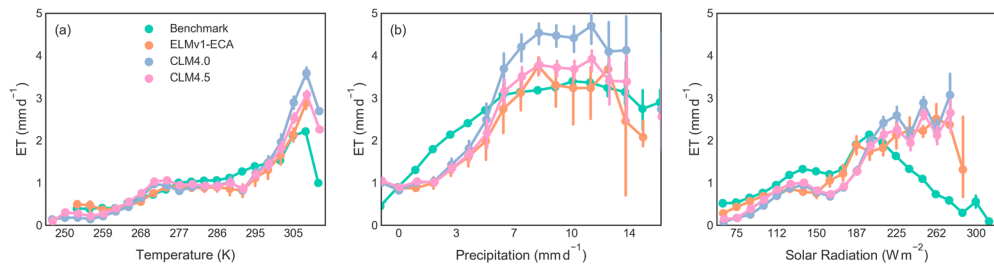


Figure 8. Empirical relationship between evapotranspiration and (a) precipitation and (b) surface air temperature.

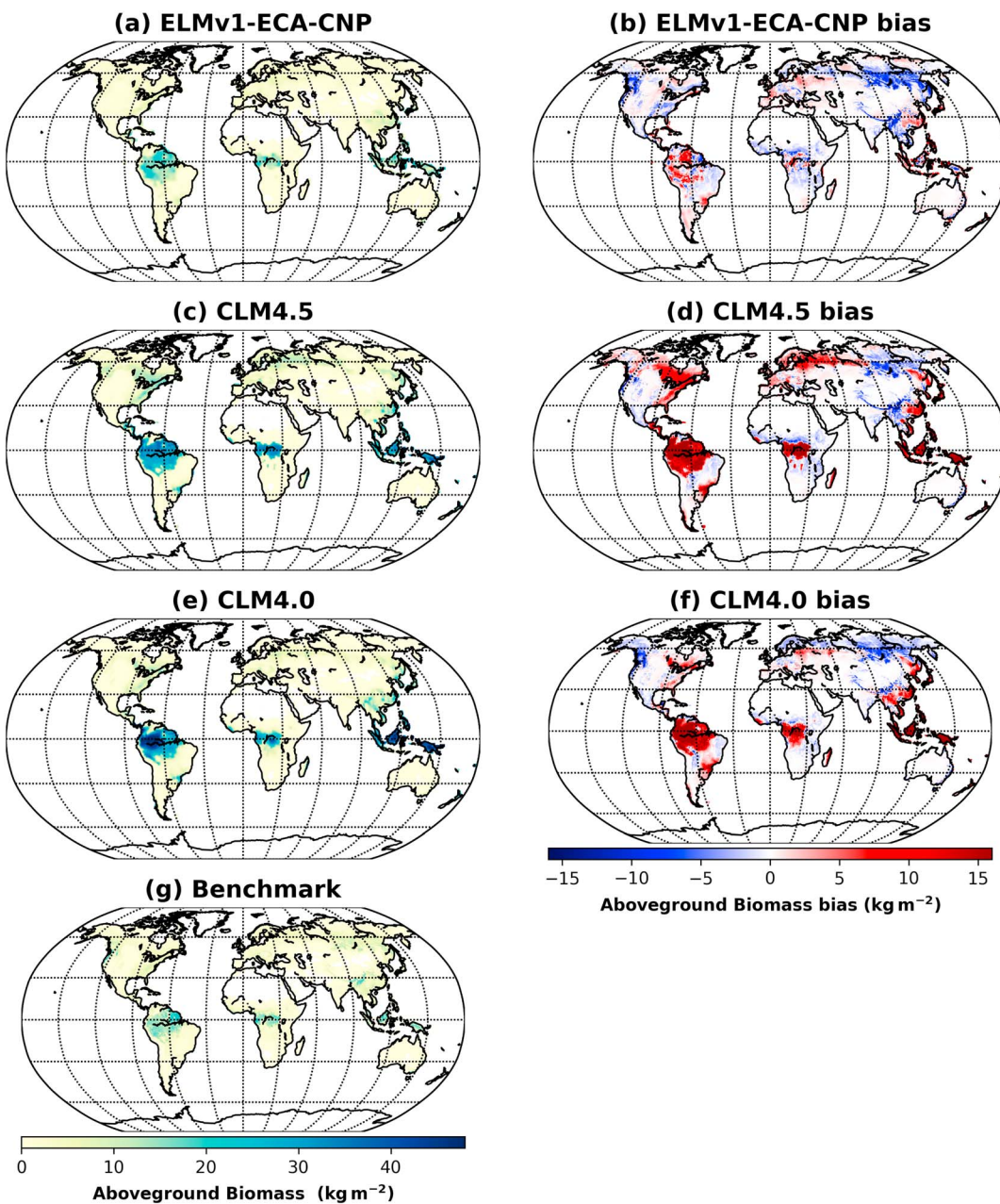


Figure 9. Global mean aboveground living biomass and bias (model-benchmark). The large bias of vegetation biomass in Community Land Model version 4.0 (CLM4.0) was partly reduced in CLM4.5 simulation, and was further reduced in Energy Exascale Earth System Model (E3SM) Land Model version 1-equilibrium chemistry approximation (ELMv1-ECA) over the tropics.

northern hemisphere tundra ecosystems, and gradually declined toward the tropical rainforest ecosystem (Figure S3). This spatial pattern reversed for leaf C to P ratio, implying that tropical ecosystems are mostly P limited. As a result of the strong P limitation over the tropics, the leaf to fine root ratio was higher over cold regions and relatively lower in tropical ecosystems (Figure S3), which generated a testable hypothesis that plants tend to allocate more carbon into fine root growth for phosphorus acquisition. Based on limited site-level estimates of forest growth in different components, the allocation into leaves is comparable to that into fine roots (Malhi et al., 2009). A comprehensive evaluation of the ELMv1-ECA dynamic allocation scheme will require more observation data.

Table 2
ILAMB Benchmarking Score for Aboveground Living Biomass

Model	Period mean [Pg]	Bias score	Spatial distribution score	Overall score
Benchmark	354			
ELMv1-ECA	431	0.63	0.84	0.74
CLM4.5-BGC	730	0.43	0.54	0.48
CLM4.0-CN	702	0.45	0.46	0.45

Note. The bold numbers represent the best model.

Abbreviations: CLM4.5-BGC, Community Land Model version 4.5 BGC; ELMv1-ECA, Energy Exascale Earth System Model (E3SM) Land Model version 1-equilibrium chemistry approximation; ILAMB, International Land Model Benchmarking.

Although lacking large-scale observational benchmarks for nutrient cycles, it is still important to document critical nutrient cycle fluxes and compare them with values reported in previous work. In ELMv1-ECA, global mean N₂ fixation rate during the last five decades of the simulation (1961–2010) of 175 Tg N/year compared well with global N₂ fixation estimates from the literature (100–290 Tg N/year (Cleveland et al., 1999), 138 Tg N/year (Galloway et al., 2004); Figure S4). ELMv1-ECA simulation also revealed an increasing N₂ fixation trend, which could be explained by the relief of energetic constraints on nitrogenous activity by warming and stimulation by progressively stronger P limitation (Houlton et al., 2008). Global nitrogen loss through hydrological (NO₃ leaching and runoff) and gaseous (N₂O emissions) pathways were estimated to be 48 and 11 Tg N/year based on Galloway et al. (2004). ELMv1-ECA simulated (Figure S4) mean annual gaseous losses (10 Tg N/year) were consistent with published estimates (Galloway et al., 2004; Mosier, 1994), while ELMv1-ECA underestimated hydrological NO₃ losses (17 Tg/year), partly because the agriculture land N leaching loss was not considered in the simulation. Spatially, most of the gaseous N losses occurred over tropical regions, where high biological N₂ fixation occurs. This pattern implies a relatively open N cycle in tropical ecosystems. In contrast to the primary N input from biological N₂ fixation (Figure S4a), the primary P input due to weathering declined over time from 1961 to 2010 due to insufficient replenishment of parent material (39 Tg P/year; Figure S5). Taken together, terrestrial ecosystems progressively became less N limited and more P limited from 1961 to 2010, and these N and P imbalances may continue or increase over the 21st century. Consistent with this argument, ELMv1-ECA showed that during the last five decades, leaf C:P ratio changed more significantly than leaf C:N ratio (Figure S6). Tropical system C:P ratio was higher than the initial base value, while nontropical system C:P ratio was similar to the initial base value. In contrast, tropical system C:N ratio was similar to the initial base value, while nontropical system C:N was much higher than the initial base value (comparing the locations of boxes and the beginning of the line with same color). The simulated P leaching losses were relatively stable, with a mean annual loss of 13 Tg P/year, which agreed with estimates from other modeling studies, for example, 14 Tg P/year in Wang et al. (2010). Moreover, ELMv1-ECA simulated a significantly lower P weathering input over tropical ecosystems due to depleted parent material (Yang et al., 2013), compared with temperate ecosystems. ELMv1-ECA also had a less prominent tropical–temperate contrast in P leaching losses, compared with P weathering.

Table 3
ILAMB Benchmarking Score for Soil Carbon Stock Down to 1-m Depth With NCSCD and HWSD Soil Data sets

Model	NCSCD score	HWSD score	Overall score
ELMv1ECA	0.71	0.72	0.71
CLM4.5-BGC	0.61	0.51	0.55
CLM4.0-CN	0.29	0.58	0.45

Note. The bold numbers represent the best model.

Abbreviations: CLM4.5-BGC, Community Land Model version 4.5 BGC; ELMv1-ECA, Energy Exascale Earth System Model (E3SM) Land Model version 1-equilibrium chemistry approximation; HWSD, Harmonized World Soil Database; ILAMB, International Land Model Benchmarking; NCSCD, The Northern Circumpolar Soil Carbon Database.

3.6. Future Improvement Suggested by Benchmarking

Through benchmarking the ELMv1-ECA predictions, we conclude that the new model captures global patterns of major carbon-related quantities better than either of its baseline predecessor models. However, our benchmarking also reveals important biases against observations and provides information on model mechanisms (and observational deficiencies) that may be responsible for the biases.

Plants open stomata to fix atmospheric CO₂ and thereby lose water to the atmosphere. The water use efficiency (WUE; i.e., the ratio between carbon fixed and water transpired) is a critical physiological characteristic important for ecosystem interactions with the atmosphere. Over the Amazon rainforest and Northern boreal forest ecosystem, ELMv1-ECA

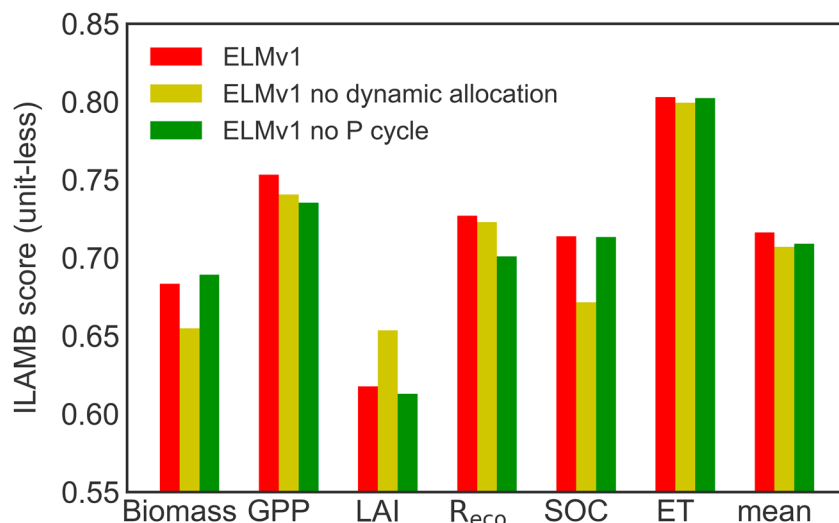


Figure 10. International Land Model Benchmarking (ILAMB) evaluation of individual components in Energy Exascale Earth System Model (E3SM) Land Model version 1-equilibrium chemistry approximation (ELMv1-ECA). The y axis starts from 0.55 for better visualization. Compared with the full ELMv1-ECA model (red bars), the dynamic allocation scheme (yellow bars) mostly affects biomass, leaf area index (LAI), and soil organic carbon (SOC), state variables, while the phosphorus cycle (green bars) reduces model performance of carbon fluxes (GPP: gross primary productivity; R_{eco} : total ecosystem respiration).

consistently overestimates GPP (Figure 2) and underestimates ET (Figure 7), leading to an overestimate of ecosystem scale WUE. This WUE overestimation implies that modeled Amazon rainforests and Northern boreal forests are unrealistically conservative in their water use.

ELMv1-ECA improved carbon cycle predictions unevenly across latitude. A relatively large improvement is found in the tropics, implying that the improved phosphorus limitation, nutrient competition, and dynamic allocation in ELMv1-ECA are mechanistically important for lowland tropical carbon dynamics (Figure 2). However, phosphorus limitation and dynamic allocation may play different roles for different aspects of the carbon cycle (Figure 10). Furthermore, a reliable GPP estimate should be consistent with reasonable LAI estimates, or a model could reproduce observed GPP by overestimating LAI and underestimating the leaf level carbon fixation rate (or vice versa). ELMv1-ECA's predicted LAI bias (Figure 5) is relatively low in the tropics, particularly given the likely underestimate of tropical MODIS LAI associated with, for example, cloud contamination and MODIS algorithm saturation (Heiskanen et al., 2012). ELMv1-ECA overestimated LAI in general, but relative biases were lower than either baseline model (Figure 5 and Table 1). We note that although the absolute bias is small, the relative GPP bias ((model minus observations)/observation) in the pan-Arctic region was similar (67.5–90°N ~14%), compared with pan-Tropical region (-23.5 S –23.5°N ~16%) and larger than temperate region (23.5–67.5°N ~4%), given that observed arctic GPP is low.

It is challenging to reasonably predict soil carbon stocks. Todd-Brown et al. (2013) showed that most of the carbon-only land models overestimated SOC stocks, while the only model in the CMIP5 analysis that represented nitrogen cycling substantially underestimated SOC stocks (CCSM4). ELMv1-ECA estimated the global SOC stock to 1-m depth to be ~1,100 Pg C, which is lower than that of CLM4.5-BGC (~1,800 Pg C) and higher than that of CLM4.0-CN (~600 Pg C; benchmark 1,270 Pg C; Todd-Brown et al., 2013). Predicted SOC stocks result from the balance between soil carbon inputs and losses through respiration (erosion and leaching are not yet represented). Although there is no global data set of litter inputs, we have higher confidence in this predicted flux compared with the base models because of the overall improvement in predicted carbon cycle metrics in ELMv1-ECA (Figures 2–6). In addition, the soil carbon turnover rates applied in ELMv1-ECA have been evaluated against some radiocarbon observations (Koven et al., 2013). In other work, we have extended this type of evaluation with a rich data set of soil radiocarbon profiles (Chen et al., 2019).

ELMv1-ECA introduced many new parameters to support model development. Although most of the parameters are directly measurable and largely constrained by existing databases (Tables S1 and S2), we

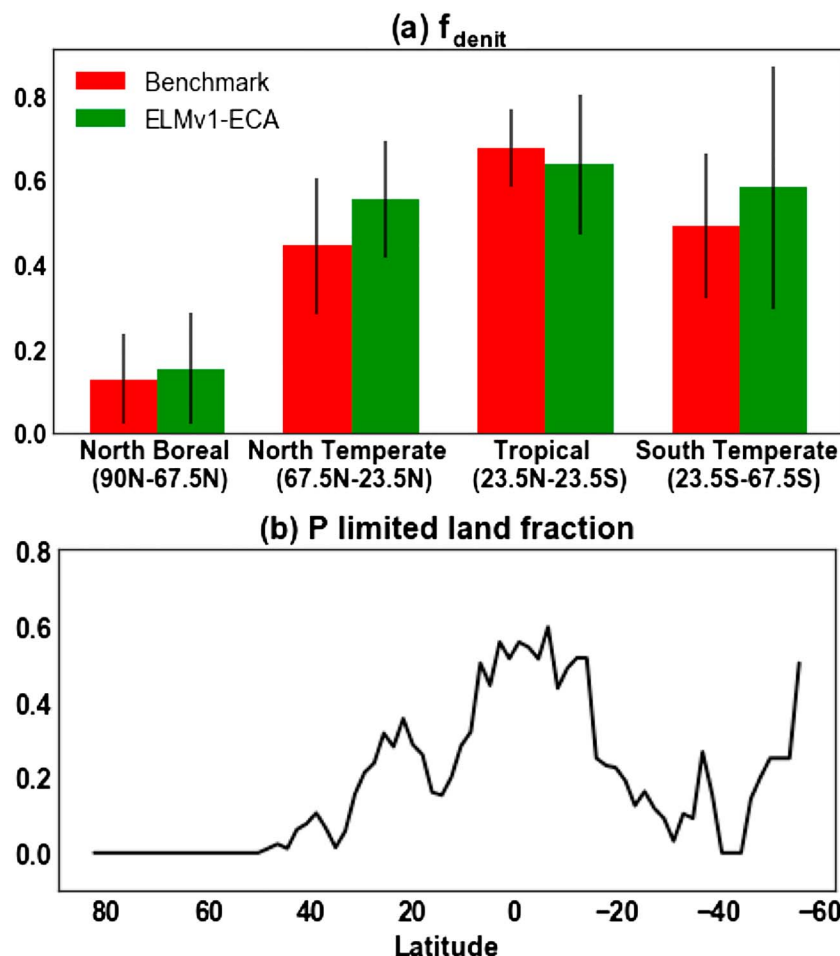


Figure 11. Latitudinal distribution of Energy Exascale Earth System Model (E3SM) Land Model version 1-equilibrium chemistry approximation (ELMv1-ECA) modeled: (a) f_{denit} (fraction of denitrification gaseous N loss to total gaseous and hydrological N loss; Houlton et al., 2015); (b) leaf C:N:P stoichiometry based evaluation of terrestrial ecosystem P limitation (Wang et al., 2010).

acknowledge potential tradeoffs of benefits associated with more mechanistic representations versus parameter uncertainty. Future work will be focused on parameter sensitivity and uncertainty quantification.

3.7. Suggestions and Limitations

Land models have been intensively evaluated from in situ to global scales, but commonly against only a few metrics in each evaluation. We suggest that the land-modeling community will benefit from systematic benchmarking against multiple data sets during model development. A disaggregated (i.e., against individual observations) and overall (i.e., combining the evaluation into a single metric) model benchmarking approach allows a consistent and repeatable evaluation of model improvements over time. Considering a wide range of metrics also informs whether changes to a model that improve a given process representation simultaneously degrade other model predictions.

We here focus our analysis on the present-day carbon cycle; more work is needed to evaluate nitrogen (N) and phosphorus (P) cycle dynamics against observational benchmarks (Bouskill et al., 2014). We suggest several nutrient cycle benchmarks urgently needed for land model development that will be integrated in a future version of ILAMB. First, global patterns of N and P fluxes, including the major nutrient input fluxes of N_2 fixation (Cleveland et al., 1999) and phosphatase activity, induced phosphorus input flux (Margalef et al., 2017). Second, isotopic tracer studies (e.g., ^{15}N and ^{33}P) are particularly useful to inform partitioning of N and P between plants and microbes, a key determinant of ecosystem C dynamics (Kuzyakov & Xu,

2013), and relative competitiveness of individual competitors (F Chapin & Bloom, 1976; Keuper et al., 2017; Zhu, Iversen, et al., 2016; Zhu & Riley, 2015; Zhu et al., 2017; Zhu, Riley, et al., 2016). Third, transient responses of the carbon cycle to nutrient availability can provide insight into nutrient limitation effects. In this sense, N and P fertilization experiments (LeBauer & Treseder, 2008), especially those that span multiple years, and FACE experiments (Zaehle et al., 2014), are particularly useful to inform carbon-nutrient interactions.

4. Conclusions

In this study, we show new developments in the E3SM land model (ELMv1-ECA) in terms of nitrogen and phosphorus cycles and their coupling with carbon dynamics. ELMv1-ECA has several new features in terms of nutrient dynamics and carbon-nutrient coupling that are conceptually different from its predecessors (CLM4.0-CN and CLM4.5-BGC). We benchmark ELMv1-ECA, CLM4.0-CN, and CLM4.5-BGC carbon cycle predictions using the ILAMB (International Land Model Benchmarking) package and conclude that ELMv1-ECA robustly represents the present-day carbon cycle by comparison with observed gross primary productivity, total ecosystem respiration, LAI, ET, vegetation biomass, and soil carbon stocks. The new model is a substantial improvement compared to its predecessor models. We also show that model benchmarking against multiple data sets is helpful and conclude that continuously benchmarking throughout model development can help improve land model performance.

Acknowledgments

This research was supported by Energy Exascale Earth System Modeling (E3SM, <https://e3sm.org/>) Project and the Reducing Uncertainties in Biogeochemical Interactions through Synthesis and Computation (RUBISCO) Scientific Focus Area, which are sponsored by the Earth and Environmental Systems Modeling (EESM) Program under the Office of Biological and Environmental Research of the U.S. Department of Energy Office of Science. Lawrence Berkeley National Laboratory (LBNL) is managed by the University of California for the U.S. Department of Energy under contract DE-AC02-05CH11231. Oak Ridge National Laboratory (ORNL) is managed by UT-Battelle, LLC, for the U.S. Department of Energy under contract DE-AC05-00OR22725. All data are available at figshare data repository: https://figshare.com/articles/ilamb-ELMECA-data_zip/5722369. The E3SM model code is available at <https://e3sm.org/>.

References

- Bader, D., Collins, W., Jacob, R., Jones, P., Rasch, P., Taylor, M., et al. (2014). Accelerated climate modeling for energy: Project strategy and initial implementation plan. ACME Council, Department of Energy, 25 p, edited.
- Baldocchi, D. D. (2003). Assessing the eddy covariance technique for evaluating carbon dioxide exchange rates of ecosystems: Past, present and future. *Global Change Biology*, 9(4), 479–492. <https://doi.org/10.1046/j.1365-2486.2003.00629.x>
- Beer, C., Reichstein, M., Tomelleri, E., Ciais, P., Jung, M., Carvalhais, N., et al. (2010). Terrestrial gross carbon dioxide uptake: Global distribution and covariation with climate. *Science*, 329(5993), 834–838. <https://doi.org/10.1126/science.1184984>
- Bouskill, N. J., Riley, W. J., & Tang, J. Y. (2014). Meta-analysis of high-latitude nitrogen-addition and warming studies implies ecological mechanisms overlooked by land models. *Biogeosciences*, 11(23), 6969–6983. <https://doi.org/10.5194/bg-11-6969-2014>
- Chapin, F., & Bloom, A. (1976). Phosphate absorption: Adaptation of tundra graminoids to a low temperature, low phosphorus environment. *Oikos*, 27, 111–121.
- Chapin, F. S., Bloom, A. J., Field, C. B., & Waring, R. H. (1987). Plant responses to multiple environmental factors. *Bioscience*, 37(1), 49–57. <https://doi.org/10.2307/1310177>
- Chen, J., Zhu, Q., Riley, W. J., He, Y., Randerson, J. T., & Trumbore, S. (2019). Comparison with global soil radiocarbon observations indicates needed carbon cycle improvements in the E3SM land model. *Journal of Geophysical Research: Biogeosciences*. <https://doi.org/10.1029/2018JG004795>
- Cleveland, C. C., Townsend, A. R., Schimel, D. S., Fisher, H., Howarth, R. W., Hedin, L. O., et al. (1999). Global patterns of terrestrial biological nitrogen (N₂) fixation in natural ecosystems. *Global Biogeochemical Cycles*, 13(2), 623–645. <https://doi.org/10.1029/1999GB900014>
- Collier, N., Hoffman, F. M., Lawrence, D. M., Keppel-Aleks, G., Koven, C. D., Riley, W. J., et al. (2018). The International Land Model Benchmarking (ILAMB) system: Design, theory, and implementation. *Journal of Advances in Modeling Earth Systems*, 10(11), 2731–2754. <https://doi.org/10.1029/2018MS001354>
- Collier, N., Hoffman, F. M., Mu, M., Randerson, J. T., and Riley, W. J. (2016). International land Model Benchmarking (ILAMB) Package v002_00Rep., BGCF-DATA (Biogeochemistry (BGC) Feedbacks).
- De Kauwe, M. G., Disney, M. I., Quaife, T., Lewis, P., & Williams, M. (2011). An assessment of the MODIS collection 5 leaf area index product for a region of mixed coniferous forest. *Remote Sensing of Environment*, 115(2), 767–780. <https://doi.org/10.1016/j.rse.2010.11.004>
- Del Grosso, S. J., Parton, W. J., Mosier, A. R., Ojima, D. S., Kulmala, A. E., & Phongpan, S. (2000). General model for N₂O and N₂ gas emissions from soils due to denitrification. *Global Biogeochemical Cycles*, 14(4), 1045–1060. <https://doi.org/10.1029/1999GB001225>
- Dirmeyer, P. A., Gao, X., Zhao, M., Guo, Z., Oki, T., & Hanasaki, N. (2006). GSWP-2: Multimodel analysis and implications for our perception of the land surface. *Bulletin of the American Meteorological Society*, 87(10), 1381–1398. <https://doi.org/10.1175/BAMS-87-10-1381>
- Elser, J. J., Bracken, M. E. S., Cleland, E. E., Gruner, D. S., Harpole, W. S., Hillebrand, H., et al. (2007). Global analysis of nitrogen and phosphorus limitation of primary producers in freshwater, marine and terrestrial ecosystems. *Ecology Letters*, 10(12), 1135–1142. <https://doi.org/10.1111/j.1461-0248.2007.01113.x>
- Eyring, V., Bony, S., Meehl, G. A., Senior, C. A., Stevens, B., Stouffer, R. J., & Taylor, K. E. (2016). Overview of the Coupled Model Intercomparison Project Phase 6 (CMIP6) experimental design and organization. *Geoscientific Model Development*, 9(5), 1937–1958. <https://doi.org/10.5194/gmd-9-1937-2016>
- Falkowski, P., Scholes, R. J., Boyle, E. A., Canadell, J., Canfield, D., Elser, J., et al. (2000). The global carbon cycle: A test of our knowledge of Earth as a system. *Science*, 290(5490), 291–296.
- Finzi, A. C., Norby, R. J., Calfapietra, C., Gallet-Budynek, A., Gielen, B., Holmes, W. E., et al. (2007). Increases in nitrogen uptake rather than nitrogen-use efficiency support higher rates of temperate forest productivity under elevated CO₂. *Proceedings of the National Academy of Sciences*, 104(35), 14014–14019. <https://doi.org/10.1073/pnas.0706518104>
- Friedlingstein, P., Joël, G., Field, C. B., & Fung, I. Y. (1999). Toward an allocation scheme for global terrestrial carbon models. *Global Change Biology*, 5(7), 755–770. <https://doi.org/10.1046/j.1365-2486.1999.00269.x>

- Galloway, J. N., Dentener, F. J., Capone, D. G., Boyer, E. W., Howarth, R. W., Seitzinger, S. P., et al. (2004). Nitrogen cycles: Past, present, and future. *Biogeochemistry*, 70(2), 153–226. <https://doi.org/10.1007/s10533-004-0370-0>
- Gardesröm, P., & Wigge, B. (1988). Influence of photorespiration on ATP/ADP ratios in the chloroplasts, mitochondria, and cytosol, studied by rapid fractionation of barley (*Hordeum vulgare*) protoplasts. *Plant Physiol.*, 88(1), 69–76. <https://doi.org/10.1104/pp.88.1.69>
- Gerber, S., Hedin, L. O., Oppenheimer, M., Pacala, S. W., & Shevliakova, E. (2010). Nitrogen cycling and feedbacks in a global dynamic land model. *Global Biogeochemical Cycles*, 24, GB1001. <https://doi.org/10.1029/2008GB003336>
- Goll, D. S., Brovkin, V., Parida, B. R., Reick, C. H., Kattge, J., Reich, P. B., et al. (2012). Nutrient limitation reduces land carbon uptake in simulations with a model of combined carbon, nitrogen and phosphorus cycling. *Biogeosciences*, 9(9), 3547–3569. <https://doi.org/10.5194/bg-9-3547-2012>
- Heiskanen, J., Rautiainen, M., Stenberg, P., Möttus, M., Vesanto, V.-H., Korhonen, L., & Majasalmi, T. (2012). Seasonal variation in MODIS LAI for a boreal forest area in Finland. *Remote Sens. Environ.*, 126, 104–115. <https://doi.org/10.1016/j.rse.2012.08.001>
- Hengl, T., de Jesus, J. M., MacMillan, R. A., Batjes, N. H., Heuvelink, G. B., Ribeiro, E., et al. (2014). SoilGrids1km—global soil information based on automated mapping. *PLoS One*, 9(8). <https://doi.org/10.1371/journal.pone.0105992>
- Hiederer, R., & Köchy, M. (2011). Global soil organic carbon estimates and the harmonized world soil database. *EUR*, 79, 25225.
- Hoffman, F. M., Koven, C. D., Keppel-Aleks, G., Lawrence, D. M., W. J. Riley Ahlström, G. Abramowitz, et al. (2017). International Land Model Benchmarking (ILAMB) 2016 Workshop Report, Technical Report DOE/SC-0186Rep., USDOE Office of Science, Washington, DC (United States).
- Hoffman, F. M., Randerson, J. T., Arora, V. K., Bao, Q., Cadule, P., Ji, D., et al. (2014). Causes and implications of persistent atmospheric carbon dioxide biases in Earth system models. *Journal of Geophysical Research: Biogeosciences*, 119, 141–162. <https://doi.org/10.1002/2013JG002381>
- Houghton, R. A. (2007). Balancing the global carbon budget. *Annual Review of Earth and Planetary Sciences*, 35(1), 313–347. <https://doi.org/10.1146/annurev.earth.35.031306.140057>
- Houlton, B. Z., Marklein, A. R., & Bai, E. (2015). Representation of nitrogen in climate change forecasts. *Nature Climate Change*, 5(5), 398–401. <https://doi.org/10.1038/nclimate2538>
- Houlton, B. Z., Wang, Y.-P., Vitousek, P. M., & Field, C. B. (2008). A unifying framework for dinitrogen fixation in the terrestrial biosphere. *Nature*, 454(7202), 327–330. <https://doi.org/10.1038/nature07028>
- Hugelius, G., Bockheim, J. G., Camill, P., Eberling, B., Grosse, G., Harden, J. W., et al. (2013). A new data set for estimating organic carbon storage to 3 m depth in soils of the northern circumpolar permafrost region. *Earth System Science Data*, 5(2), 393–402. <https://doi.org/10.5194/essd-5-393-2013>
- Hungate, B. A., Dukes, J. S., Shaw, M. R., Luo, Y., & Field, C. B. (2003). Nitrogen and climate change. *Science*, 302(5650), 1512–1513. <https://doi.org/10.1126/science.1091390>
- Kattge, J., Knorr, W., Raddatz, T., & Wirth, C. (2009). Quantifying photosynthetic capacity and its relationship to leaf nitrogen content for global-scale terrestrial biosphere models. *Global Change Biology*, 15(4), 976–991. <https://doi.org/10.1111/j.1365-2486.2008.01744.x>
- Keuper, F., Dorrepaal, E., van Bodegom, P. M., van Logtestijn, R., Venhuizen, G., van Hal, J., & Aerts, R. (2017). Experimentally increased nutrient availability at the permafrost thaw front selectively enhances biomass production of deep-rooting subarctic peatland species. *Global Change Biology*, 23(10), 4257–4266. <https://doi.org/10.1111/gcb.13804>
- Koerselman, W., & Meuleman, A. F. M. (1996). The vegetation N: P ratio: A new tool to detect the nature of nutrient limitation. *Journal of Applied Ecology*, 33, 1441–1450.
- Koven, C. D., Riley, W. J., Subin, Z. M., Tang, J. Y., Torn, M. S., Collins, W. D., et al. (2013). The effect of vertically resolved soil biogeochemistry and alternate soil C and N models on C dynamics of CLM4. *Biogeosciences*, 10(11), 7109–7131. <https://doi.org/10.5194/bg-10-7109-2013>
- Kuzyakov, Y., & Xu, X. (2013). Competition between roots and microorganisms for nitrogen: Mechanisms and ecological relevance. *New Phytologist*, 198(3), 656–669. <https://doi.org/10.1111/nph.12235>
- Lamarque, J. F., Kiehl, J. T., Brasseur, G. P., Butler, T., Cameron-Smith, P., Collins, W. D., et al. (2005). Assessing future nitrogen deposition and carbon cycle feedback using a multimodel approach: Analysis of nitrogen deposition. *Journal of Geophysical Research*, 110, D19303. <https://doi.org/10.1029/2005JD005825>
- Le Quéré, C., Andrew, R. M., Canadell, J. G., Sitch, S., Korsbakken, J. I., Peters, G. P., et al. (2016). Global Carbon Budget 2016. *Earth System Science Data*, 8, 605–649. <https://doi.org/10.5194/essd-8-605-2016>
- LeBauer, D. S., & Treseder, K. K. (2008). Nitrogen limitation of net primary productivity in terrestrial ecosystems is globally distributed. *Ecology*, 89(2), 371–379. <https://doi.org/10.1890/06-2057.1>
- Luo, Y. Q., Randerson, J. T., Abramowitz, G., Bacour, C., Blyth, E., Carvalhais, N., et al. (2012). A framework for benchmarking land models. *Biogeosciences*, 9(10).
- Mahowald, N., Jickells, T. D., Baker, A. R., Artaxo, P., Benitez-Nelson, C. R., Bergametti, G., et al. (2008). Global distribution of atmospheric phosphorus sources, concentrations and deposition rates, and anthropogenic impacts. *Global Biogeochemical Cycles*, 22, GB4026. <https://doi.org/10.1029/2008GB003240>
- Malhi, Y., Saatchi, S., Girardin, C., & Aragão, L. (2009). *The production, storage, and flow of carbon in Amazonian forests*. Amazonia and Global Change (pp. 355–372).
- Mao, J., Ribes, A., Yan, B., Shi, X., Thornton, P. E., Séférian, R., et al. (2016). Human-induced greening of the northern extratropical land surface. *Nature Climate Change*, 6, 959–963.
- Margalef, O., Sardans, J., Fernández-Martínez, M., Molowny-Horas, R., Janssens, I., Ciais, P., et al. (2017). Global patterns of phosphatase activity in natural soils. *Scientific Reports*, 7.
- Medlyn, B. E., De Kauwe, M. G., Zaehle, S., Walker, A. P., Duursma, R. A., Luus, K., et al. (2016). Using models to guide field experiments: A priori predictions for the CO₂ response of a nutrient-and water-limited native Eucalypt woodland. *Global Change Biology*, 22(8), 2834–2851. <https://doi.org/10.1111/gcb.13268>
- Miralles, D., Holmes, T., De Jeu, R., Gash, J., Meesters, A., & Dolman, A. (2011). Global land-surface evaporation estimated from satellite-based observations. *Hydrology and Earth System Sciences*, 15(2), 453–469. <https://doi.org/10.5194/hess-15-453-2011>
- Mosier, A. (1994). Nitrous oxide emissions from agricultural soils. *Fertilizer Research*, 37(3), 191–200. <https://doi.org/10.1007/BF00748937>
- Myhre, G., Highwood, E. J., Shine, K. P., & Stordal, F. (1998). New estimates of radiative forcing due to well mixed greenhouse gases. *Geophys. Res. Lett.*, 25(14), 2715–2718. <https://doi.org/10.1029/98GL01908>
- Norby, R. J., De Kauwe, M. G., Domingues, T. F., Duursma, R. A., Ellsworth, D. S., Goll, D. S., et al. (2016). Model-data synthesis for the next generation of forest free-air CO₂ enrichment (FACE) experiments. *New Phytologist*, 209(1), 17–28. <https://doi.org/10.1111/nph.13593>

- Norby, R. J., DeLucia, E. H., Gielen, B., Calfapietra, C., Giardina, C. P., King, J. S., et al. (2005). Forest response to elevated CO₂ is conserved across a broad range of productivity. *Proceedings of the National Academy of Sciences of the United States of America*, 102(50), 18,052–18,056. <https://doi.org/10.1073/pnas.0509478102>
- Norby, R. J., Warren, J. M., Iversen, C. M., Medlyn, B. E., & McMurtrie, R. E. (2010). CO₂ enhancement of forest productivity constrained by limited nitrogen availability. *Proceedings of the National Academy of Sciences*, 107(45), 19,368–19,373. <https://doi.org/10.1073/pnas.1006463107>
- Oleson, K., Lawrence, D. M., Bonan, G. B., Drewniak, B., Huang, M., Koven, C. D., et al. (2013). Technical description of version 4.5 of the Community Land Model (CLM) Technical Note NCAR/TN-503+STR. <https://doi.org/10.5065/D6RR1W7M>
- Penuelas, J., Poulter, B., Sardans, J., Ciais, P., van der Velde, M., Bopp, L., et al. (2013). Human-induced nitrogen–phosphorus imbalances alter natural and managed ecosystems across the globe. *Nature Communications*, 4.
- Petit, J.-R., Jouzel, J., Raynaud, D., Barkov, N. I., Barnola, J. M., Basile, I., et al. (1999). Climate and atmospheric history of the past 420,000 years from the Vostok ice core, Antarctica. *Nature*, 399(6735), 429–436. <https://doi.org/10.1038/20859>
- Reich, P. B., & Hobbie, S. E. (2013). Decade-long soil nitrogen constraint on the CO₂ fertilization of plant biomass. *Nature Climate Change*, 3(3), 278–282. <https://doi.org/10.1038/nclimate1694>
- Reich, P. B., Hobbie, S. E., Lee, T., Ellsworth, D. S., West, J. B., Tilman, D., et al. (2006). Nitrogen limitation constrains sustainability of ecosystem response to CO₂. *Nature*, 440(7086), 922–925. <https://doi.org/10.1038/nature04486>
- Reich, P. B., Oleksyn, J., & Wright, I. J. (2009). Leaf phosphorus influences the photosynthesis–nitrogen relation: A cross-biome analysis of 314 species. *Oecologia*, 160(2), 207–212. <https://doi.org/10.1007/s00442-009-1291-3>
- Reichstein, M., Falge, E., Baldocchi, D., Papale, D., Aubinet, M., Berbigier, P., et al. (2005). On the separation of net ecosystem exchange into assimilation and ecosystem respiration: Review and improved algorithm. *Global Change Biology*, 11(9), 1424–1439. <https://doi.org/10.1111/j.1365-2486.2005.001002.x>
- Saatchi, S. S., Harris, N. L., Brown, S., Lefsky, M., Mitchard, E. T. A., Salas, W., et al. (2011). Benchmark map of forest carbon stocks in tropical regions across three continents. *Proceedings of the National Academy of Sciences*, 108(24), 9899–9904. <https://doi.org/10.1073/pnas.1019576108>
- Sharpe, P. J. H., & Rykiel, E. J. (1991). *Modelling integrated response of plants to multiple stresses, Response of plants to multiple stresses* (pp. 205–224). New York: Academic Inc Press.
- Sinha, E., Michalak, A., & Balaji, V. (2017). Eutrophication will increase during the 21st century as a result of precipitation changes. *Science*, 357(6349), 405–408. <https://doi.org/10.1126/science.aan2409>
- Tang, J. Y., & Riley, W. J. (2013). A total quasi-steady-state formulation of substrate uptake kinetics in complex networks and an example application to microbial litter decomposition. *Biogeosciences*, 10(12), 8329–8351. <https://doi.org/10.5194/bg-10-8329-2013>
- Tang, J. Y., & Riley, W. J. (2018). Predicted land carbon dynamics are strongly dependent on the numerical coupling of nitrogen mobilizing and immobilizing processes: A demonstration with the E3SM land model. *Earth Interactions*, 22(11), 1–18. <https://doi.org/10.1175/EI-D-17-0023.1>
- Taylor, K. E., Stouffer, R. J., & Meehl, G. A. (2012). An overview of CMIP5 and the experiment design. *Bulletin of the American Meteorological Society*, 93(4), 485–498. <https://doi.org/10.1175/BAMS-D-11-00094.1>
- Thornton, P. E., Lamarque, J. F., Rosenbloom, N. A., & Mahowald, N. M. (2007). Influence of carbon–nitrogen cycle coupling on land model response to CO₂ fertilization and climate variability. *Global Biogeochemical Cycles*, 21, GB4018. <https://doi.org/10.1029/2006GB002868>
- Todd-Brown, K. E., Randerson, J. T., Post, W. M., Hoffman, F. M., Tarnocai, C., Schuur, E. A., & Allison, S. D. (2013). Causes of variation in soil carbon simulations from CMIP5 Earth system models and comparison with observations. *Biogeosciences*, 10(3).
- Vitousek, P. M., Mooney, H. A., Lubchenco, J., & Melillo, J. M. (1997). Human domination of Earth's ecosystems. *Science*, 277(5325), 494–499. <https://doi.org/10.1126/science.277.5325.494>
- Walker, A. P., Beckerman, A. P., Gu, L., Kattge, J., Cernusak, L. A., Domingues, T. F., et al. (2014). The relationship of leaf photosynthetic traits—Vcmax and Jmax—to leaf nitrogen, leaf phosphorus, and specific leaf area: A meta-analysis and modeling study. *Ecology and evolution*, 4(16), 3218–3235. <https://doi.org/10.1002/ece3.1173>
- Wang, Y. P., Law, R. M., & Pak, B. (2010). A global model of carbon, nitrogen and phosphorus cycles for the terrestrial biosphere. *Biogeosciences*, 7(7), 2261–2282. <https://doi.org/10.5194/bg-7-2261-2010>
- Wieder, W., Cleveland, C. C., Smith, W. K., & Todd-Brown, K. (2015). Future productivity and carbon storage limited by terrestrial nutrient availability. *Nature Geoscience*, 8(6), 441–444. <https://doi.org/10.1038/ngeo2413>
- Woodrow, I. E., & Berry, J. A. (1988). Enzymatic regulation of photosynthetic CO₂ fixation in C3 plants. *Annu. Rev. Plant Physiol. Plant Mol. Biol.*, 39(1), 533–594. <https://doi.org/10.1146/annurev.pp.39.060188.002533>
- Wu, J., Albert, L. P., Lopes, A. P., Restrepo-Coupe, N., Hayek, M., Wiedemann, K. T., et al. (2016). Leaf development and demography explain photosynthetic seasonality in Amazon evergreen forests. *Science*, 351(6276), 972–976. <https://doi.org/10.1126/science.aad5068>
- Xia, J., & Wan, S. (2008). Global response patterns of terrestrial plant species to nitrogen addition. *New Phytol.*, 179(2), 428–439. <https://doi.org/10.1111/j.1469-8137.2008.02488.x>
- Xu, R. I., & Prentice, I. C. (2008). Terrestrial nitrogen cycle simulation with a dynamic global vegetation model. *Global Change Biology*, 14(8), 1745–1764. <https://doi.org/10.1111/j.1365-2486.2008.01625.x>
- Yang, X., Post, W. M., Thornton, P. E., & Jain, A. (2013). The distribution of soil phosphorus for global biogeochemical modeling. *Biogeosciences*, 10(4), 2525–2537. <https://doi.org/10.5194/bg-10-2525-2013>
- Yang, X., Thornton, P. E., Ricciuto, D. M., & Post, W. M. (2014). The role of phosphorus dynamics in tropical forests—A modeling study using CLM-CNP. *Biogeosciences*, 11(6), 1667–1681. <https://doi.org/10.5194/bg-11-1667-2014>
- Zaehle, S., & Dalmonech, D. (2011). Carbon–nitrogen interactions on land at global scales: Current understanding in modelling climate biosphere feedbacks. *Current Opinion in Environmental Sustainability*, 3(5), 311–320. <https://doi.org/10.1016/j.cosust.2011.08.008>
- Zaehle, S., Medlyn, B. E., De Kauwe, M. G., Walker, A. P., Dietze, M. C., Hickler, T., et al. (2014). Evaluation of 11 terrestrial carbon–nitrogen cycle models against observations from two temperate Free-Air CO₂ Enrichment studies. *New Phytologist*, 202(3), 803–822. <https://doi.org/10.1111/nph.12697>
- Zhu, Q., Iversen, C. M., Riley, W. J., Slette, I. J., & Van der Stel, H. M. (2016). Root traits explain observed tundra vegetation nitrogen uptake patterns: Implications for trait-based land models. *Journal of Geophysical Research: Biogeosciences*, 121, 3101–3122. <https://doi.org/10.1002/2016JG003554>
- Zhu, Q., & Riley, W. J. (2015). Improved modelling of soil nitrogen losses. *Nature Climate Change*, 5(8), 705–706. <https://doi.org/10.1038/nclimate2696>
- Zhu, Q., Riley, W. J., & Tang, J. (2017). A new theory of plant–microbe nutrient competition resolves inconsistencies between observations and model predictions. *Ecological Applications*, 27(3), 875–886. <https://doi.org/10.1002/eap.1490>

- Zhu, Q., Riley, W. J., Tang, J., & Koven, C. D. (2016). Multiple soil nutrient competition between plants, microbes, and mineral surfaces: Model development, parameterization, and example applications in several tropical forests. *Biogeosciences*, 12(5), 4057–4106. <https://doi.org/10.5194/bgd-12-4057-2015>
- Zhu, Q., & Zhuang, Q. (2013). Modeling the effects of organic nitrogen uptake by plants on the carbon cycling of boreal ecosystems. *Biogeosciences*, 10(8), 13,455–13,490. <https://doi.org/10.5194/bgd-10-13455-2013>